

IOWA STATE UNIVERSITY

Digital Repository

Retrospective Theses and Dissertations

Iowa State University Capstones, Theses and
Dissertations

1989

Flux quantization effects in disordered normal metal rings and superconducting networks

Qiming Li

Iowa State University

Follow this and additional works at: <https://lib.dr.iastate.edu/rtd>



Part of the [Condensed Matter Physics Commons](#)

Recommended Citation

Li, Qiming, "Flux quantization effects in disordered normal metal rings and superconducting networks " (1989). *Retrospective Theses and Dissertations*. 9214.

<https://lib.dr.iastate.edu/rtd/9214>

This Dissertation is brought to you for free and open access by the Iowa State University Capstones, Theses and Dissertations at Iowa State University Digital Repository. It has been accepted for inclusion in Retrospective Theses and Dissertations by an authorized administrator of Iowa State University Digital Repository. For more information, please contact digirep@iastate.edu.

INFORMATION TO USERS

The most advanced technology has been used to photograph and reproduce this manuscript from the microfilm master. UMI films the text directly from the original or copy submitted. Thus, some thesis and dissertation copies are in typewriter face, while others may be from any type of computer printer.

The quality of this reproduction is dependent upon the quality of the copy submitted. Broken or indistinct print, colored or poor quality illustrations and photographs, print bleedthrough, substandard margins, and improper alignment can adversely affect reproduction.

In the unlikely event that the author did not send UMI a complete manuscript and there are missing pages, these will be noted. Also, if unauthorized copyright material had to be removed, a note will indicate the deletion.

Oversize materials (e.g., maps, drawings, charts) are reproduced by sectioning the original, beginning at the upper left-hand corner and continuing from left to right in equal sections with small overlaps. Each original is also photographed in one exposure and is included in reduced form at the back of the book. These are also available as one exposure on a standard 35mm slide or as a 17" x 23" black and white photographic print for an additional charge.

Photographs included in the original manuscript have been reproduced xerographically in this copy. Higher quality 6" x 9" black and white photographic prints are available for any photographs or illustrations appearing in this copy for an additional charge. Contact UMI directly to order.

U·M·I

University Microfilms International
A Bell & Howell Information Company
300 North Zeeb Road, Ann Arbor, MI 48106-1346 USA
313/761-4700 800/521-0600

Order Number 8929159

**Flux quantization effects in disordered normal metal rings and
superconducting networks**

Li, Qiming, Ph.D.

Iowa State University, 1989

U·M·I

**300 N. Zeeb Rd.
Ann Arbor, MI 48106**

**Flux quantization effects in disordered
normal metal rings and superconducting networks**

by

Qiming Li

**A Dissertation Submitted to the
Graduate Faculty in Partial Fulfillment of the
Requirements for the Degree of
DOCTOR OF PHILOSOPHY**

Department: Physics

Major: Solid State Physics

Approved:

Signature was redacted for privacy.

In Charge of Major Work

Signature was redacted for privacy.

For the Major Department

Signature was redacted for privacy.

For the Graduate College

**Iowa State University
Ames, Iowa**

1989

TABLE OF CONTENTS

	Page
GENERAL INTRODUCTION	1
Introduction to Anderson Localization	1
Conductance Fluctuation in Mesoscopic Systems	18
Flux Quantization Effects in Superconductors	28
Explanation of the Dissertation's Format	34
PART I. QUANTUM OSCILLATIONS IN ONE-DIMENSIONAL	
METAL RINGS: AVERAGE OVER DISORDER	36
Abstract	37
Introduction	37
Results and Discussion	38
Conclusions	45
Acknowledgments	46
References	46
PART II. HALF-FLUX-QUANTUM MAGNETORESISTANCE	
OSCILLATIONS IN DISORDERED METAL RINGS	53
Abstract	54
Introduction	54
Results and Discussion	56
Conclusions	62
Acknowledgments	63
References	63

PART III. METAL-INSULATOR TRANSITION IN RANDOM	
SUPERCONDUCTING NETWORKS	69
Abstract	70
Introduction	70
Results and Discussion	71
Conclusions	80
Acknowledgments	80
References	81
SUMMARY	88
LITERATURE CITED	90
ACKNOWLEDGMENTS	94
APPENDIX. NUMERICAL METHOD OF FINITE SIZE SCALING	95

GENERAL INTRODUCTION

Introduction to Anderson Localization

The electron conduction of matter is a subject of fundamental importance in condensed matter physics. In crystalline materials, the existence of the periodic potential simplifies greatly the complexity of solving the Schrödinger equation for a macroscopic system. The wave functions of electrons are described through Bloch's theorem as plane-waves modulated by the periodic atomic lattice. The Bloch electron in a perfect periodic potential can sustain an electric current, even in the absence of any driving electric field because the momentum of electrons is conserved (translational symmetry exists). The finite electronic conductivity is entirely due to the deviation of lattice from perfect order, such as the disorder due to impurities and defects, or intrinsic deviations due to thermal vibrations of the lattice.

In the conventional semiclassical treatment, the total effects of these imperfections are simply represented in the conductivity formula of the Drude form, but now the mean free path, which is the length between successive scattering in Drude's intuitive picture, is calculated through the scattering time of independent electrons with the imperfections. Since the electrons obey Fermi statistics, only electrons within $k_B T$ of Fermi energy E_F contribute to the conductivity. At room temperature, the most important contribution to the conductivity of ordinary metals is the scattering of electrons with

phonons (thermal vibration of lattice). As the temperature is lowered, the amplitude of the lattice vibration decreases and with it the resistance drops. This decrease will continue until extremely low temperatures, when the scattering by impurities and defects begins to take over. This results in a residual resistance at $T=0$.

In the last ten years our understanding of the physics of disordered systems, in particular their transport properties, has greatly changed and substantially deepened.¹ Extensive theoretical and experimental work show that the conventional picture described above needs major modifications. It is found experimentally that contrary to the conventional theory, the resistivity increases with a decrease in temperature in many disordered metallic systems and even diverges logarithmically for a thin film. A metal-insulator phase transition, analogous to the second order phase transition, has also been found for strong disordered systems. Even more surprising was the experimental discovery that small devices are nonself-averaging in the sense that large conductance fluctuations exist from sample to sample. All these remarkable phenomena can now be understood within the framework of Anderson localization theory, which has greatly broadened our scope of understanding of the disordered materials in general.

The concept of localization was first introduced by Anderson² in 1958 in a seminal paper to describe the unusual behavior of electrons in disordered materials. The central question Anderson tried to answer was the following: What is the character of electron waves in a random potential? By random potential, we mean that at any point in space the

potential might take any of a range of values, and only the probabilities for these values are specified. In weak disordered systems, electron waves are scattered by impurities with a mean free path l . Although the momentum and the phase of electrons may be different after scattering, the amplitude of the wave function is still finite and extends into the entire system. Using a perturbation treatment, Anderson showed that this is not the only possibility. When disorder gets stronger, there could be localized states whose envelope of the wave function amplitude decays exponentially with distance. The wave function of such a state is given as

$$\Psi(r) \sim e^{-r/L_c} \quad (1.1)$$

The characteristic length L_c is called the localization length. The existence of these localized states can be easily understood in the very strong disorder limit, where the eigenstate of the electron is a bound state produced by the deep potential fluctuation. It was later rigorously shown that all states are localized in a strictly one-dimensional system,³ no matter how weak the disorder.

The existence of these localized states is also manifested in the spectrum of disordered systems. Besides the usual continuous spectrum which represents extended states, there also exist discrete singular eigenvalues which have localized wave functions. It can be argued that these two different states can not mix with each other. The energy which separates the extended states from the localized states is called

mobility edge. For localized states, diffusivity of the electron becomes zero for a macroscopic system. Therefore, at $T=0$, when the Fermi energy moves across the mobility edge, the behavior of the system will go from metallic to insulating. This phase transition is termed as Mott transition.³

The picture of localized states in disordered systems is a fundamental departure from the conventional view. It shows that important new physics comes in. A disordered system is not merely a dirty-regular one but belongs to a new class which has to be treated in a fundamentally different way. In spite of its importance as a basic notion in solid state physics, the microscopic understanding of Anderson localization has been hindered until recently by the intrinsic complexity due to randomness. A key step was established when Thouless⁴ and later Abrahams et al.⁵ developed the scaling theory of electron localization. The main idea of this theory is that one can determine whether the system is in a localized state or in an extended state by studying the dependence of its conductance on its size. This new theory of the disordered systems predicts, among other things, that all states are localized for $d=1,2$ and a phase transition between localized and extended states exists for $d=3$. This immediately stimulated a great deal of theoretical and experimental interest and resulted in a total breakthrough in the understanding of the disordered systems.

Some of the most important ideas of the scaling theory of localization were developed in the mid-70s by Thouless and co-workers.⁴

Thouless conjectured that the nature of the eigenstates of a random finite size system can be determined by the sensitivity of the energy levels to changes of the boundary conditions. In particular, the conductance is given by the ratio of the two quantities: the shift of the energy levels E_T (also called Thouless energy) of the system due to changes of boundary conditions from periodic to antiperiodic, and the averaged energy level spacing ΔE . Thouless suggested that

$$G = \frac{e^2}{h} \frac{E_T}{\Delta E} = \frac{e^2}{h} g, \quad (1.2)$$

where $g = G/(e^2/h)$ is dimensionless and is called the Thouless number.

We present below one of Thouless's heuristic arguments in obtaining Eq. (1.2). Consider a block of material of length L . The time τ_D needed for an electron wave packet to diffuse from one end of the sample to the other is given by

$$\tau_D = \frac{L^2}{D}, \quad (1.3)$$

where D is the diffusion constant related to the conductivity σ through Einstein's relation $\sigma = e^2 n(E_F) D$. τ_D will be associated with a energy level shift E_T by the uncertainty principle

$$E_T = \frac{h}{\tau_D} = \frac{h}{L^2} \frac{\sigma}{e^2} \frac{1}{n(E_F)}. \quad (1.4)$$

For a sample of size L^d , where d is the dimensionality, the density of states $n(E)$ is given by

$$n(E) = \frac{L^d}{\Delta E} \quad (1.5)$$

Hence,

$$G = \sigma L^{d-2} = \frac{e^2}{h} \frac{E_T}{\Delta E} \quad (1.6)$$

Therefore we arrive at Thouless's conjecture.

The above picture is very reasonable on the following physical ground. If $E_T \ll \Delta E$, the eigenstate energy is not perturbed by adding more blocks of the material and the eigenstate will still be confined within the region of the original block. Hence, states are localized. On the other hand, if $E_T > \Delta E$, any change in the boundary will cause the mixture of levels with the next nearby block and the final wave function extends to the next block. Hence, an extended state is inferred.

The criteria that a state becomes exponentially localized when $G \ll e^2/h$, though simple, has profound consequences. It predicts that the zero temperature resistance of a wire will decrease linearly at first with increasing length, following from Ohm's law, and once its value exceeds a critical number, the resistance will then begin to increase exponentially since the state becomes localized. At finite

temperatures, inelastic scattering due to thermal excitations will destroy the phase coherence of electron waves and the motion of the electron will become classical diffusive. Therefore, the resistance will increase linearly after the coherence length scale, a result familiar with our common experience.

Thouless's picture of the localization shows deep physical insights, but it is hard to lead to any specific detail dependences of the conductance on the size of the system. A major breakthrough came in 1980. In a famous paper Abrahams et al.⁵ proposed one parameter scaling hypothesis. The basic assumptions of the scaling theory are:

- 1) Thouless number, $g=G/(e^2/h)$, is the only relevant scaling parameter;
- 2) g for a hypercube of $(bL)^d$ is determined by g for a cube of L .
Or explicitly

$$g(bL)=f_d(b,g(L)) \quad (1.7a)$$

In a differential form,

$$\frac{d \ln g(L)}{d \ln L} = \beta_d(g(L)) \quad , \quad (1.7b)$$

where $\beta_d(g)$ is assumed to be a continuous and monotonic universal function depending only on dimensionality d .

Limiting behaviors of the β function can be obtained. In the weak disordered region, $L \gg l$ but g is still large, we know that the

macroscopic transport theory is correct. For a hypercube with length L , according to Ohm's law

$$G(L) = \sigma L^{d-2} \quad , \quad (1.8)$$

so that

$$\lim_{g \rightarrow \infty} \beta_d(g) = d-2 \quad . \quad (1.9)$$

For strong disorder, $g \ll 1$, exponential localization takes place and we expect

$$g = g_0 e^{-\alpha L} \quad , \quad (1.10)$$

so that

$$\lim_{g \rightarrow 0} \beta_d(g) = \ln \frac{g}{g_0} \quad , \quad (1.11)$$

where g_0 is the value around the transition from the extended to the localized state and is of the order of unity. A plot of the β function is shown in Figure 1. Remarkably, we see that for $d=1,2$, g always decreases with increasing L so all states are localized for a macroscopic system. On the other hand, for $d=3$ there exists an unstable fixed point at g_c . For a system with $g > g_c$, states are extended and the conductance increases to the classical value with the increase of the system size, while for a system with $g < g_c$, states are localized and eventually conductance will go to zero when the system

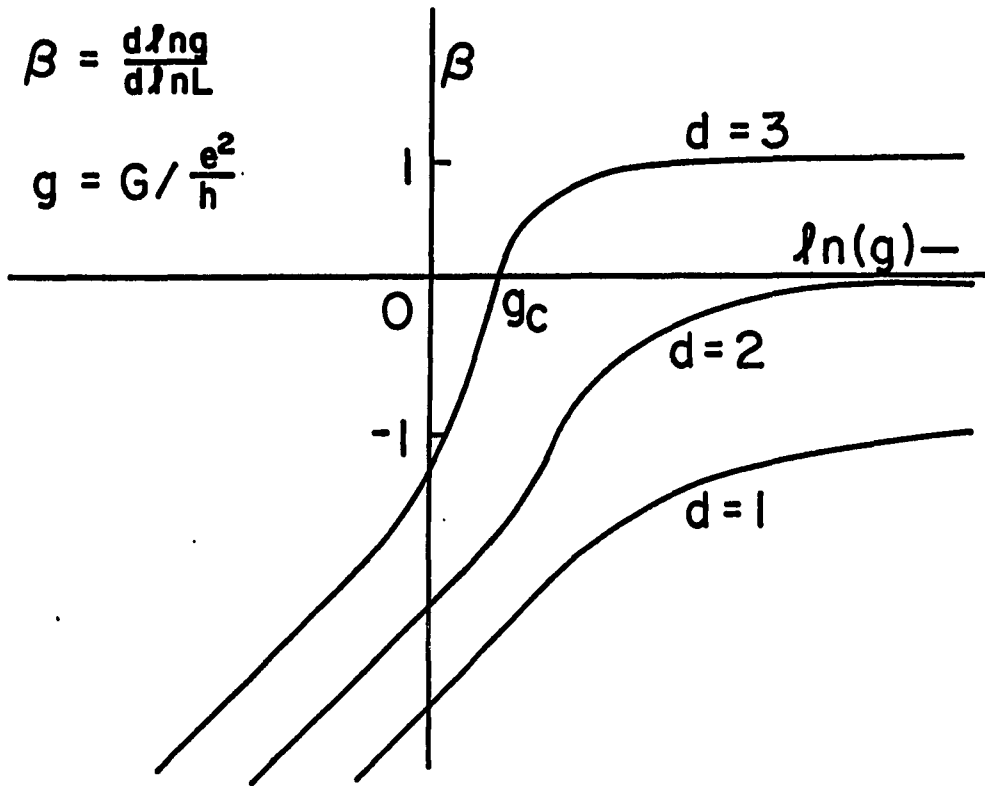


Fig. 1. The scaling function $\beta(g)$ vs the dimensionless conductance g for different dimension

size is very large. This picture of a continuous phase transition was at that time against the prevailing idea of minimum conductivity by Mott. He argued that since the smallest possible value for the mean free path is the interatomic distance, a minimum conductivity must exist of the order of $\sigma_c = e^2 a^{2-d}/h$. Many careful experiments have been done and they failed to find the existence of such a minimum value in support of the predictions of scaling theory.

It is important to point out that Thouless's number, g , is not the only choice for the scaling. Indeed, many well-behaved characteristic quantities can be used as the scaling parameter. A different scaling function could be found which should essentially give the same localization behavior as the β function. Mackinnon and Kramer⁶ used the localization length of a finite size system as the scaling variable and found a universal scaling curve numerically. The β function can then be related and explicitly evaluated (see Appendix).

Scaling theory states that once the conductance at one length is known, one can predict, in principle, the conductance at any other length scale from the scaling function. To get an explicit expression, however, complicated calculations are involved. When the disorder is relative weak, a diagrammatic perturbation theory is used and in two dimensions produces the well-known logarithmic divergence correction to the conductivity. The correction is largely due to a phenomenon called weak localization,⁷ which results from the constructive interference of different electron trajectories in quantum diffusion. Let us

illustrate this idea in detail, because it is also important to the understanding of the conductance oscillations in disordered materials.

Consider a particle initially at point A. We ask, what is the probability that later in time this particle will be found at point B? There are many possible trajectories that the particle can take to go from A to B (Figure 2a). Each path is associated with a probability amplitude A_i . Therefore the total probability is given by

$$P = \left| \sum_i A_i \right|^2 = \sum_i |A_i|^2 + \sum_{i \neq j} A_i A_j^* \quad . \quad (1.12)$$

Conventional transport theory assumes that collisions are uncorrelated so the interference term, the second term on the RHS of Eq. (1.12), is neglected. This is normally allowed even for quantum transport, because different paths arrive at B with different amplitudes and different phases due to the random multiple scattering events. On the average, this would result in a total cancellation of interference effects. There is, however, one particular exception to this conclusion, namely if point A and B coincide (Figure 2b). Then, every trajectory has a conjugated partner which is the time reversal event and has exactly the same phase shift. In this case, the interference term in Eq. (1.12) will contribute to P the same amount $\sum_i |A_i|^2$, so the probability that an electron comes back to the origin is doubled. This constructive interference leads to the enhancement of the backscattering, hence to a decrease in the diffusion of the electron and therefore to possible localization. It turns out that this quantum

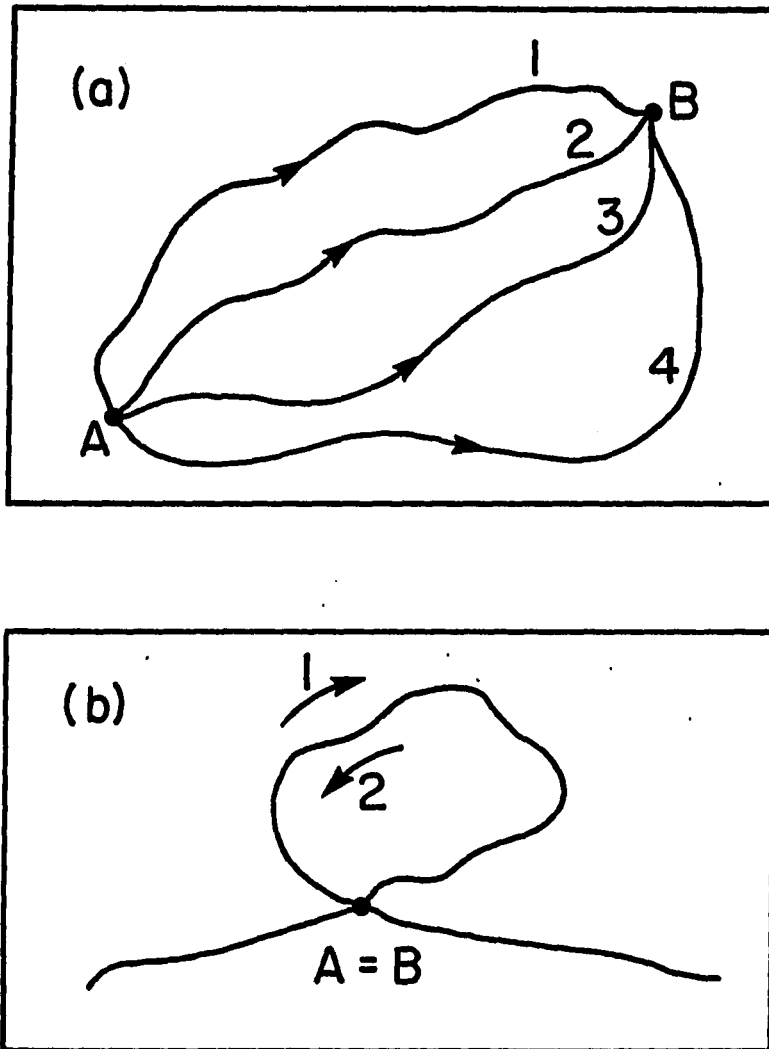


Fig. 2. Paths of a particle:

- a) several possible paths of a particle diffusing from A to B;
- b) The constructive interference of two time-reversal paths.

correction is very important in weak disordered systems in $d=3$, and it even diverges with the system size in $d=1,2$ because all trajectories contribute equally in $d=1,2$.

Until now we have assumed that phase coherence is maintained over the entire sample. It was earlier believed that an electron loses its phase memory within the mean free path, typically of the order of 100 Å. Only much later it was realized that elastic scattering by static disorder, such as impurities (nonmagnetic), does not destroy phase coherence, it merely shifts the phase by a fixed amount. Only inelastic scattering events, such as the electron-phonon interaction, are responsible for the destruction of the phase coherence. The length that an electron diffuses before losing its memory completely is called phase coherence length. It is roughly given by

$$L_\phi = L_{in} = (D\tau_{in})^{1/2} \quad (1.13)$$

This length could be as large as 1 μm at liquid-helium temperature.

The inelastic scattering length provides a upper length limit for quantum corrections of the weak localization due to the backscattering. The lower cutoff length is naturally the mean free path. This leads to¹

$$\frac{\delta\sigma}{\sigma_0} = \begin{array}{lll} (L_{in}/l)^{1/2} & d=1 & (1.14a) \\ \ln(L_{in}/l) & d=2 & (1.14b) \\ (L_{in}/l)^{-1/2} & d=3 & (1.14c) \end{array}$$

where $\sigma_0 = ne^2\tau/m$ is the Boltzmann conductivity, named because it is a direct result of the Boltzmann transport theory. We see from Eqs. (1.14a-c) that quantum corrections are very important in $d=1,2$, since $L_{in} \gg l$.

We have explicitly assumed that time reversal symmetry exists in our systems. Either external magnetic field or internal magnetic impurities certainly destroys such a symmetry. The magnetic field introduces a phase shift for every A_i in Eq. (1.12). The phase shifts for the two time-reversal paths have the opposite sign, hence these two trajectories are not in phase anymore. This destruction of the constructive interference, hence the weakening of the localization of electrons due to the external magnetic field in disordered systems, is responsible for a general phenomenon called negative magnetoresistance, namely, increasing of the conductance with increasing magnetic field. The phase shift by the magnetic flux also has important consequences in the electron conductance of small mesoscopic systems.

The above weak scattering picture shows how important it is to consider the quantum mechanical corrections in different physical quantities. Such basic physical notions have already existed thirty years ago. In 1957, Landauer⁸ made a major contribution to the understanding of electron conduction and coherence by introducing a simple relation between the conductance of a 1-d system to the transmission coefficient. The so-called Landauer's formula is

$$G = \frac{e^2 T}{h R} \quad (1.15)$$

Instead of appealing to the complicated transport theory, Landauer considered the simplest situation of a wire connected to heat baths at the two ends (Fig. 3). The phases of the electrons are randomized only in the reservoirs. All the scatterings in the wire are elastic and can be represented simply by a total transmission coefficient T and total reflection coefficient $R=1-T$. Now imagine that the chemical potential difference of the two reservoirs is $\delta\mu$. Then, the extra density of electrons on one side will be

$$\delta n = \frac{dn}{dE} e \delta\mu \quad (1.16)$$

On the other hand,

$$\delta n = n_l - n_r = \frac{J_l + J_r}{v_l} - \frac{J_o + J_{l'}}{v_r} = 2R(J_l - J_{l'})/v \quad (1.17)$$

where J_l , J_r , J_o , and $J_{l'}$ are the particle currents associated with and directions l , r , o , and l' , respectively (see Fig. 3). v_r and v_l are the electron velocities. $v_r = v_l = v$. The total electric current

$$I = e(J_l - J_r) = e(J_o - J_{l'}) = e(J_l - J_{l'})T \quad (1.18)$$

so the conductance

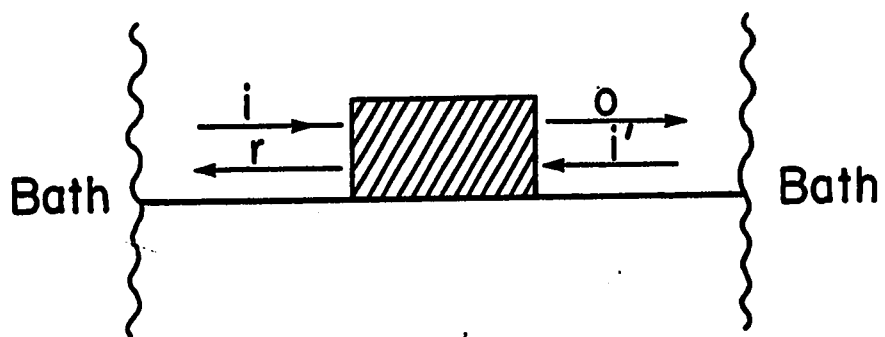


Fig. 3. The Landauer geometry for transport through a barrier.

$$G = \frac{I}{\delta\mu} = \frac{T}{2R} \frac{dn}{dE} e^2 v = \frac{e^2}{h} \frac{T}{R} \quad (1.19)$$

where relation $v = \frac{2\pi dE}{h dk} = 2 \frac{dE}{dn}$ for 1-d has been used.

More complicated derivations⁹ starting from Kubo's formula exist. We emphasize here that quantum coherence of electrons is implicitly assumed in all derivations.

Landauer's formula provides not only a conceptional breakthrough, but also a convenient way to calculate the conductance of a disordered system, which is much more difficult to calculate than the transmission coefficient, even numerically. Strictly speaking, Landauer's formula can only be applied to the 1-d system. Many attempts have been made to generalize it to higher dimensions. Some basic assumptions, however, must be made for the equilibrium condition in the system. Moreover, all these formulas are complicated and lack of a simple picture. An example is the multichannel formula obtained by Anderson et al.⁹

$$G = \frac{e^2}{h} \frac{n}{\sum_{\alpha=1}^n} \frac{\sum_{\beta=1}^n |t_{\alpha\beta}|^2}{1 - \sum_{\beta=1}^n |t_{\alpha\beta}|^2}, \quad (1.20)$$

where $t_{\alpha\beta}$ is the transmission amplitude from channel α to channel β , and n is the total number of channels. Channels can be classified by

quantum numbers in perfect leads connected to the disordered system.

For large numbers of channels we expect $|t_{\alpha\beta}|^2 \sim 1/n$, hence

$$G = \frac{e^2}{h} \sum_{\alpha} \sum_{\beta} |t_{\alpha\beta}|^2 = \frac{e^2}{h} \text{Tr} (t^+ t) \quad . \quad (1.21)$$

Eq. (1.21) was first obtained by Economou and Soukoulis¹⁰ in $d=1$ and by Fisher and Lee¹⁰ in $d=2$

We also mention that a multichannel and multiprobe formula has been derived by Buttiker.¹¹ This formula found interesting applications in the asymmetric fluctuations of the conductance and in the understanding of the quantum Hall effects.

Conductance Fluctuation in Mesoscopic Systems

Now that we have the basic concepts of the quantum coherence and electron localization, we should see how these ideas can be applied to real systems and tested experimentally. We know that for lengths longer than the phase coherence length, the diffusion of the electron becomes classical. Therefore, the quantum conduction can be best demonstrated in small devices with a length scale comparable to the phase coherence length. Advances in modern lithography have made it possible to fabricate devices in the submicron scale. The physics in such systems is dominated by the quantum coherence of electron waves. Many unexpected and very interesting phenomena show up in such a system. Stone¹² first proposed to call it a mesoscopic system. These

systems consist of large numbers of atoms, but still do not have the self-averaging property of a typical macroscopic system. The most experimentally studied mesoscopic systems are wires,¹³ rings,¹⁴ and MOSFET (metal-oxide-semiconductor field-effect transistor).¹⁵ Studies of mesoscopic structures have revealed sample-dependent intrinsic fluctuations in transport properties, which are surprisingly sensitive to magnetic fields. These fluctuations are not noise, since they are reproducible under exactly the same physical conditions. They are, in fact, signatures of the microscopic configurations of the sample. The origin of fluctuations can be understood in a way through Landauer's formula. The transmission coefficient of an electron in a disordered system can vary greatly, depending on the exact configuration of the random potential and the energy of the electron. Therefore, the conductance of such a system should show large sample-dependent fluctuations. In real experiments, the fluctuations can be probed through varying magnetic fields (the reason that the magnetic fields can change the conductance of such a mesoscopic system is anticipated from Eq. (1.12)) or in the case of MOSFET, by varying the Fermi energy. The overall effects are very similar in these different cases.

Using the perturbation technique, Lee and Stone and later Al'tshuler et al. were able to show that fluctuations in mesoscopic systems have universal features.⁶ The proposed universal conductance fluctuation hypothesis states that, in the metallic regime the amplitude of the conductance fluctuations, ΔG (rms value), is a universal constant and is independent of the sample size, degree of the

disorder, and the dimensionality as long as the phase coherence is maintained over the entire sample:

$$\langle \Delta G \rangle \sim \alpha \frac{e^2}{h} \quad \text{for } L < L_\phi \quad . \quad (1.22)$$

The constant α is in the order of unity and later found to weakly depend on the dimensionality. The length-independent conductance fluctuations might be expected from the scaling theory of localization at least in two cases: the weak disordered regime in $d=2$ and the phase transition regime in $3-d$. In both cases, the β function is very small and the conductance is almost length independent. Hence, length-independent conductance fluctuations are consistent with the scaling theory.

For systems with $L \gg L_\phi$, fluctuations of the conductance within a subsystem of size L_ϕ are correlated, but fluctuations for different subsystems are not. This will introduce an average due to the random phase for the oscillation of different subsystems. The relative fluctuation amplitude will decrease according to the law of large numbers:

$$\frac{\Delta G}{G} \sim \left(\frac{L}{L_\phi} \right)^{d/2} \frac{\Delta G(L_\phi)}{G(L_\phi)} \quad , \quad (1.23)$$

where $(L/L_\phi)^d$ gives the total number of the uncorrelated subsystems.

To test the idea of the universal conductance fluctuation, we must consider the complications of an average procedure due to finite temperatures and finite magnetic fields. There should always exist some characteristic scale such that electrons with parameters differing by more than this amount will exhibit different interference patterns. This correlation range can be approximately determined by requiring the phase difference of two paths, with parameters different by this correlation range, equal to 2π . For example, the time needed for an electron to travel a sample length L is $\Delta t = L^2/D$, where D is the diffusion constant. Thus the phase difference of two electrons with energy difference ΔE is approximately $\Delta \phi = 2\pi \Delta E \Delta t / h$. Hence the energy correlation range for the system is simply the Thouless energy, $E_c = \hbar D / L^2$. The magnetic field correlation range B_c can also be obtained from similar arguments. It is the field when the total flux through the sample $\Phi = B_c W L$ is $\Phi_0 = h/e$, or equivalently, when the phase difference of the two outermost paths due to the magnetic field is 2π . Either way we get $B_c = \Phi_0 / W L$. Both analytical and numerical studies^{12,16,17} of the correlation functions give $E_c = (\hbar D / L^2)$ and $B_c = 1.2 \Phi_0 / L W$ for a sample of length L and width W . For $k_B T < E_c$, there will be no effect of the temperature on the quantum transport properties. If $k_B T > E_c$, the effect of the temperature average¹⁶ reduces the zero temperature quantum fluctuation amplitude $\Delta G(T=0)$ stochastically by a factor $(E_c / k_B T)^{1/2}$.

The universal conductance fluctuation hypothesis has been confirmed experimentally in many systems, generally with $L > L_\phi$ and

through use of Eq. (1.23).¹⁸ Experiments for systems with $L < L_\phi$, however, show quite unexpected novel phenomena. Instead of the universal conductance fluctuation of the order h/e^2 , the amplitude of the resistance fluctuations is found to be a constant for $L < L_\phi$.¹⁹ This implies that $\Delta G = \Delta R/R^2$ can change by orders of magnitude. One can argue this is due to the nonlocal effect of the measurements. Since the coherence of electrons is always maintained within L_ϕ even if $L < L_\phi$, the leads must become a part of the system under consideration. There are contributions from the conductance fluctuations of the leads. This nonlocal effect is clearly demonstrated in a setup where the conductance of a wire is measured with a small metal ring dangling on a sidebranch.¹⁸ Although no current flows through the ring, an oscillation with the flux period of the ring as h/e nevertheless appears in the conductance of the wire. Currently, there is still no satisfactory theory to account for fluctuations of this type besides numerical simulations.

Another interesting discovery of the experiments is that four terminal measurements show asymmetric fluctuations upon reversing the magnetic field direction. This apparent violation of the so-called Onsager relation, $\sigma_{ij}(H) = \sigma_{ij}(-H)$, can be explained solely by considering probe configurations of four terminal measurements. Buttiker¹¹ has developed a multiprobe Landauer type of formula. In his theory, there exist two types of oscillations: one symmetrical and the other antisymmetrical with respect to the change of the field direction. This prediction is supported by a detailed analysis of

experimental data.²⁰ This multiprobe formula is also used recently in connection with the quantum Hall effect in disordered systems.

While the origin of the nonlocal and the asymmetric effects is still under debate, there are important phenomena that have been studied and well understood in recent years. One is the periodic conductance oscillation of the Aharonov-Bohm type in a multiconnected normal metal system. These samples offer much cleaner signals and are better systems in which to test the theoretical ideas of the universal conductance fluctuation and the quantum phase coherence of electrons. In the original experiment suggested by Aharonov and Bohm²¹ in 1959, an electron beam (in vacuum) is split coherently so that it travels from a common source to a common detector by two different paths which enclose a magnetic flux. Although the electrons do not experience any field, their interference patterns are modulated periodically by a flux change $\Phi_0 = h/e$ (A-B effect). This experimental fact, the vector potential will affect the phase of an electron wave function with observable consequences even when the electron is restricted to the regions of space where the electric and magnetic intensities vanish, is a manifest of the radical importance of vector potential in quantum mechanics. Al'tshuler, Aronov, and Spivak²² (AAS) pointed out that this effect should also be observable in the case of electrons in dirty metal. Sharvin and Sharvin²³ are the first to demonstrate, indeed, such an experiment was possible. In their experiment, the conductance of a normal metal hollow cylinder was found to oscillate in the magnetic field with a period $\Phi_0/2$, the same as found in the case of

superconductors. This half-quantum-flux period oscillation is, in fact, exactly predicted by the AAS theory.²² Earlier attempts to repeat this experiment on a single Au ring, however, failed to find half-flux oscillations¹⁴ (this was later attributed to the existence of magnetic impurities). Later, using a single Ag ring, Chandrasekhar et al. were the first to show that both half-flux and full-flux oscillations exist.²⁴ The $h/2e$ oscillation disappears after some characteristic field, while the h/e oscillation persists to field as large as 8 Tesla in Au rings. Besides periodic oscillations, there also exist background fluctuations.

The $h/2e$ oscillations are hard to be understood from the formalism²⁵ starting with Landauer's formula. This theory predicts that h/e oscillations should always dominate and is unable to explain the absence of h/e oscillation in the cylinder. All these apparent paradoxes have their origin in the lack of self-averaging in mesoscopic systems. The h/e oscillations come from the direct interference of electrons in the two branches, while the $h/2e$ oscillations origin in the interference of two time-reversal processes, similar to the interference of the backscattering in the weak localization. These conjugated waves effectively circulate the ring twice; therefore, the oscillation period is $h/2e$. Exactly how these two different processes interplay was controversial at the early stage of the investigation. The major difference between the two theories is that, in the AAS theory, ensemble averages have been taken. Li and Soukoulis showed that even for a single ring, average over the phase of transmission

amplitude leads to complete $h/2e$ oscillation.²⁶ Hence the key lies in the process of averaging.

There are different kinds of averaging: 1) the random average of different uncorrelated segments of length L_ϕ for a large system; 2) the thermal average of different channels of energy width E_c for $k_B T > E_c$; and 3) the magnetic field effect due to the finite width of the quasi-one-dimensional system. The first two processes have similar effects: they tend to decrease the relative amplitude of the h/e oscillations but have no effect on the $h/2e$ oscillations because no matter what the phase of the individual wave, the two conjugated waves are always in phase. Hence, the conductance at $B=0$ is always at a maximum. The magnetic field in the sample, however, kills the $h/2e$ oscillation quickly. The reason that the $h/2e$ oscillation is more sensitive to the magnetic field is because magnetic flux generally destroys the constructive interference. The only situation that the two conjugated waves can be in phase is when their phase difference due to the magnetic flux is a multiple of 2π . But it is impossible to have all the pairs in phase at a constant field, since different trajectories would enclose different fluxes. It is this destruction of the constructive interference which leads to the disappearance of the $h/2e$ oscillations. The h/e oscillation, on the other hand, is the interference result of many trajectories. Thus, any additional shifts of phase due to different amount of flux enclosed will not change the oscillation amplitude by much. Therefore, the h/e oscillation is more robust. The field for the disappearance of the $h/2e$ oscillation can be

estimated as the field at which the flux on the arms of the ring is approximately $\Phi_0 = h/e$. At this field, the phase differences between the inner most path and outer most path due to magnetic flux is 4π .

Therefore, we obtain a coherent picture of the Aharonov-Bohm effect which can be best summarized mathematically as

$$\Delta G(H) = C(H) + A \frac{e^2}{h} \cos\left(\frac{e}{h}\Phi + \phi_1\right) + B \frac{e^2}{h} \cos\left(\frac{2e}{h}\Phi\right) \quad (1.25)$$

$$A = A_0 \left(\frac{E_c}{k_B T}\right)^{1/2} \exp(-\pi r/L_\phi)$$

$$B = B_0 \exp(-2\pi r/L_\phi)$$

where A represents the amplitude of the h/e fluctuations, B the amplitude of the $h/2e$ oscillations, and C the aperiodic background fluctuations due to the finite width of the rings. A_0 and B_0 are constants of order of unity. Φ is the magnetic flux through the hole of the ring, and ϕ_1 is a random offset which shifts the phase of the oscillations at zero magnetic field and can be any number between 0 and 2π . In Eq. (1.25), a factor due to thermal average is introduced. An additional factor is also introduced to take into account the probability that the electrons arrive coherently, which decrease exponentially once the radius r is larger than L_ϕ . The $T^{-1/2}$ dependence on temperatures has been confirmed on wires and rings.¹⁸

For a network of rings with radius of a ring $r \sim L_\phi$ but the separation of rings $L_d > L_\phi$, we expect no correlations between the resistance oscillation patterns of different rings. Hence, the amplitude of the h/e oscillation $\Delta R_{h/e}(N) \sim N^{1/2} \Delta R_{h/e}(1)$ from the law of large numbers, and the amplitude of the $h/2e$ oscillation $\Delta R_{h/2e}(N) \sim N \Delta R_{h/2e}(1)$ since the $h/2e$ amplitude simply adds. Using $R(N) = NR(1)$ and $\Delta G = \Delta R/R^2$, we obtain finally the following relation for the relative amplitude of the oscillations:

$$\frac{\Delta G_{h/e}(N)}{G} = \frac{1}{N^{3/2}} \frac{\Delta G_{h/e}(1)}{G(1)} \quad (1.26a)$$

and

$$\frac{\Delta G_{h/2e}(N)}{G} = \frac{1}{N} \frac{\Delta G_{h/2e}(1)}{G(1)}, \quad (1.26b)$$

where N is the number of rings in the network. $\Delta G(1)$ is given by Eq. (1.25). This relation has also been confirmed by experiments for a series of connected rings.²⁷ Li and Soukoulis have numerically simulated this experiment²⁸ (see Part II). They found, however, the ratio A/B is inversely proportional to N rather than $N^{1/2}$ as predicted in Eqs. (1.26a,b) and also found in the experiment. This still lacks an analytical explanation. Presumably, phase coherence is larger than the inter-ring distance in the simulations of Li and Soukoulis.

Flux Quantization Effects in Superconductors

The recently discovered flux effect on multiconnected metal networks discussed above has its counterpart in superconductors: the flux quantization effect. The effect of the magnetic field on a superconductor has long been an active field. In fact, even before the development of the microscopic theory, London²⁹ pointed out that $h/2e$ should be the flux quanta. Byers and Yang, and Onsager show this is directly connected with the pairing of electrons.³⁰ The beautiful demonstration of flux quantization in 1961 by Deaver and Fairbank by the measurement of the magnetic moment through a hollow superconducting cylinder³¹, showed once again the vital importance of the vector potential in the quantum mechanical world. In the ingenious work of Little and Parks,³² the oscillations of the superconducting transition temperature of a cylinder as a function of magnetic flux through the hole was also inferred through the oscillation of the normal resistance near the phase transition. These superconductor oscillations can be well understood within the framework of the well-known phenomenological phase transition theory of Ginzburg-Landau. In recent years considerable attention has been devoted to the study of disordered superconductors.³³ In the case of strong disordered superconductors, a model of Josephson coupling arrays with random coupling constant has been used.³⁴ It turns out that this model³⁴ shows very interesting complex behavior, which has also been seen in the area of spin glasses.

However, we will concentrate on another model which primarily deals with inhomogeneous superconductors of multiple connected micrnetworks.

de Gennes and Alexander have done pioneer work in the field of multiple connected superconducting networks.³⁵ The system under investigation can be a real ordered fractal geometry like the Sierpinski gasket³⁶ or a disordered system which exhibits fractal properties, for example, a percolating network.³⁷ Here, fractal can be loosely defined as an object which shows self-similarity up to a length scale. The dimension that is associated with the growth of the mass M with respect to the length is called fractal dimension D_f of the object, $M \sim L^{D_f}$. D_f is generally different from the Euclidian dimension d . Percolating networks are generated by randomly removing some bonds with a given probability $q=1-p$. There is a phase transition at a critical value, p_c , called percolation threshold, above which an infinite cluster exists with probability one. Percolating clusters show fractal behaviors within the length scale ξ . The coherence length ξ grows like $|p-p_c|^{-\nu}$. Many critical indices can be related by the critical phenomena theory.³³ For example, the resistance of such a network at the normal state increases as $|p-p_c|^{-\nu}$, when approaching p_c from above.

Now consider the effect of the magnetic field on such a superconducting percolating network with $p > p_c$. Following de Gennes and Alexander, consider Ginzburg-Landau free energy on a thin strand

$$F = A |\Delta|^2 + \frac{1}{2} B |\Delta|^4 + C |u \cdot [\nabla - \frac{2e}{h} A] \Delta|^2, \quad (1.27)$$

where Δ is the order parameter and u is a unit vector along the strand. Equation (1.27) leads to the Ginzburg-Landau (GL) equation

$$\left\{ \frac{1}{\xi_s^2} + \left[i \frac{\partial}{\partial s} - \kappa \right]^2 + b |\Delta|^2 \right\} \Delta = 0, \quad (1.28)$$

where $s = (u \cdot r)$, $\kappa = u \cdot A / \Phi_0$ and $\xi_s^2 = -C/A \sim T_c D_0 / (T_c - T)$. D_0 is the diffusion constant on the strand. The critical field can be calculated through $H_{c2} = \Phi_0 / (2\pi \xi_s^2)$.

Equation (1.28) is generally difficult to solve, due to the nonlinearity. If we are interested only in what happens near the transition, where order parameters are expected to vanish, the nonlinear term can be neglected. However, this may be inappropriate in some cases, as will be discussed later.

Solving the linearized G-L equation on a single strand and using a "Kirchoff" matching condition on the derivatives at the nodes, we obtain a set of coupled linear equations:³⁵

$$-\Delta_i \sum_j \cot \theta_{ij} + \sum_j \Delta_j e^{i\gamma_{ij}} / \sin \theta_{ij} = 0, \quad (1.29)$$

where Δ_i is the order parameter at node i , $\theta_{ij} = L_{ij} / \xi_s$ is the bond length between nodes i and j divided by the coherence length, and $\gamma_{ij} = \oint A \cdot dl / \Phi_0$. For a system with the same bond length $L_{ij} = L$, Equation (1.29) can be written as

$$-\Delta_i z_i \cos(L/\xi_S) + \sum_j^{z_i} \Delta_j e^{i\gamma_{ij}} = 0 \quad (1.30)$$

where z_i is the number of bonds connected to node i .

The above equation is exactly the Schrödinger equation of a tight binding Hamiltonian for a disordered electron system. The transition to the superconducting state is determined by the appearance of first eigenstate with nonzero order parameter, which corresponds to the band edge of the electronic system. The band structure of this equation has been studied in detail by Hofstadter³⁸ for an ordered regular 2-d lattice in the context of the electron motion in an external magnetic fields. It was found that singular features show up at rational values of Φ/Φ_0 , with the largest features at $\Phi/\Phi_0=1/2$. This is an indication that the flux lattice finds a commensurate configuration on arrays. In superconducting networks, these features show up in the form of dips at the T_c -H phase boundary. When disorder is introduced, the translation symmetry is destroyed and loops of different sizes can not satisfy flux quantization conditions simultaneously. Therefore, those features should gradually disappear.

The edge state of Eq. (1.30) can be found exactly by direct diagonalization of the Hamiltonian or by utilizing the Sturm sequence method. The phase boundary can then be determined. On the other hand, it seems that the presence of the first state alone is not enough to guarantee a superconducting state on a macroscopic system. The extended or localized nature of the solution also plays an important role. It is well known that the states at the band edge are, in

general, extremely localized and less populated.³⁹ This means that the superconducting order parameter for such a state is not zero only at a small region of the system confined within the range of the localization length. Thus the entire system may not become superconducting at all. To have a true superconducting state, either the density of those localized edge states must be large enough so states localized at different positions can tunnel to each other, or the order parameter function Δ_1 must be more or less extended. On the other hand, an extended state is sufficient to have the entire system go superconducting. Hence, the real phase boundary must lie between the first state and the mobility edge. If this is indeed the case, then the nonlinear term may not be negligible. While detailed study along this line of thinking has just began, primary results already indicate some experimental support.⁴⁰

By studying the percolating random superconducting networks, some of the very important ideas can be tested. If the superconducting coherent length is larger than the percolation coherent length, $\xi_s > \xi_p \propto (p-p_c)^{-\nu}$, the lattice can be thought as homogenous. In this case, the normal diffusion relation $\xi_s = D\tau_{GL}(T)$ holds, where $\tau_{GL} = \pi\hbar/8k_B(T_c - T)$. This leads to a linear dependence of H_{c2} on $\Delta T_c = T_c - T$

$$\Delta T_c \sim \xi_s^2 \sim H_{c2} \quad . \quad (1.31)$$

For $\xi_s < \xi_p$, however, the fractal geometry shows up and the lattice is inhomogenous. There exist anomaly diffusions in such a system

$$\langle x^2 \rangle \sim t^{D_f/d_f} = t^{1/(1+\theta/2)}, \quad (1.32)$$

where D_f is the fractal dimension and d_f is the fracton dimensionality, $d_f=4/3$ according the Orbach-Alexander conjecture. θ is anomaly diffusion exponent. Hence $\xi_s^2 \sim \tau_{GL}^{1/(1+\theta/2)}$. This leads to

$$\Delta T_c \propto H^{1+\theta/2} \quad (1.33)$$

so there is a dimensionality crossover from $\Delta T_c \propto H$ to $\Delta T_c \propto H^{1+\theta/2}$ when ξ_s is changed.

Another important relation is the dependence of the slope of the phase trajectory at $\xi_s = \xi_p$,

$$\left. \frac{dH_c}{dT} \right|_{T_c} = \frac{\phi_0}{2\pi} \left. \frac{d\xi_s^{-2}}{dT} \right|_{T_c} \propto \xi_s^\theta \propto (p-p_c)^{-\nu \theta} \propto (p-p_c)^{-\kappa} \quad (1.34)$$

where $\kappa = \nu\theta$. Theoretical values of κ range from 0.6 to 1.1.

The predicted crossover has not been observed yet. Only the homogenous regimes are found.³⁷ The experimental determination of exponent κ is also inconclusive.³⁷

Explanation of the Dissertation's Format

This thesis follows the Alternate Thesis Format which permits the inclusion of papers submitted or to be submitted to scholarly journals. The research in all three parts was suggested by Dr. C. M. Soukoulis and performed under his supervision.

The general introduction gives an overview to the field of electron localization and the physics of mesoscopic systems. Basic physical pictures, rather than rigorous but more complicated mathematical formalism, are presented. In Part I, a single disordered metal ring under magnetic field is studied through the calculation of the total transmission coefficient. The importance of the ensemble averaging is pointed out to obtain the $h/2e$ oscillation of the AAS type. In Part II, the effect of averaging on the amplitude and the period of the conductance oscillation in metal rings are studied numerically, by using the most reliable method of the finite size scaling. The universal conductance hypothesis is also checked in these systems. Part III is aimed at the understanding of the metal-insulator transition in random superconducting networks. The phase boundaries of both the site and the bond superconducting percolation networks are obtained. The mobility edges are obtained numerically for different fields and concentrations of nodes for the site percolation networks. The effects of localization and its implication to experimental measurements are discussed. The Summary discusses what we have achieved through these studies.

Part I has been published in Physical Review B, as a Rapid Communications.²⁶ Part II has been published in Physical Review Letters.²⁸ Some material of Part III have been published in Physical Review B, as a Rapid Communications.⁴¹

PART I.

QUANTUM OSCILLATIONS IN ONE-DIMENSIONAL METAL RINGS:

AVERAGE OVER DISORDER

Abstract

We study the Aharonov-Bohm effect in single normal-metal rings and show that averaging the transmission coefficient T over disorder gives oscillations with a period of a half-flux quantum. As the elastic scattering gets stronger, the periodicity of oscillation of the conductance, which is related to T , gradually changes to a full-flux quantum, in agreement with recent experiments.

Introduction

There have been intense theoretical and experimental efforts in recent years to understand the behavior of conductance of normal metal conductors at low temperatures. Magnetoresistance oscillations of Aharonov-Bohm effect type in disordered rings and cylinders with flux period $hc/2e$ were first predicted by Al'tshuler, Aronov, and Spivak (AAS),¹ and have been verified experimentally for disordered cylinders by several groups.²⁻⁵ Experiments on small rings, on the other hand, showed complicated features. Until recently, no periodic oscillations had been clearly observed in single-metal rings. However, Webb, Washburn, Umbach, and Laibowitz⁶ have observed signals of oscillations with period hc/e in small gold rings, and very recently Chandrasekhar, Rooks, Wind, and Prober⁷ have unambiguously observed $hc/2e$ oscillations at low magnetic fields and weaker hc/e oscillations at higher magnetic fields, on single aluminum and silver rings.

The AAS theory, which predicts $hc/2e$ oscillations that decay rapidly at high fields, is based on the weak localization theory of the ensemble-averaged magnetoresistance.⁸ Carini, Muttalib, and Nagel⁹ have also predicted $hc/2e$ oscillations and argued that the origin of these oscillations of the conductance could be traced to the existence of degeneracies and time-reversal invariance of the Hamiltonian after ensemble averaging. An alternative approach,¹⁰⁻¹² based on calculating the transmission coefficient, gives a fundamental period of hc/e in rings at zero temperature. Although higher harmonics do exist, they become dominant only at special conditions and are not equivalent to the effect predicted by AAS.¹ No ensemble average is taken in this theory.¹⁰⁻¹² It was suggested^{12,13} that $hc/2e$ contribution could become dominant in the multichannel case due to the random contribution associated with flux-independent phases. In addition, in very small samples there is the extra complication of aperiodic fluctuations added to the magnetoresistance.¹⁴

Results and Discussion

In the present paper, we will first give an explicit formula of the transmission coefficient, which is related to the conductance by the Landauer's formula,^{11,12} for a symmetric normal-metal ring. Then we will show that in the weak scattering limit the conductance is a periodic function of the flux through the hole in the conductor with $hc/2e$ period after averaging over the phases of the scatterers. We

will also show that increasing scattering will destroy the $hc/2e$ oscillations, and the period will change to hc/e , in agreement with the latest experiments.

Following Buttiker, Imry, and Landauer,¹¹ we describe a metal ring by two effective parallel elastic scatterers with two leads. The leads can be described by an S matrix which relates the amplitudes of the three incoming waves to the three amplitudes of the outgoing waves. The matrix S has to be unitary and symmetric due to the physical requirement of probability conservation and time-reversal invariance. A simple choice that S is real and symmetric with respect to the two branches of the circle is given by¹¹

$$S = \begin{pmatrix} -(a+b) & \epsilon^{1/2} & \epsilon^{1/2} \\ \epsilon^{1/2} & a & b \\ \epsilon^{1/2} & b & a \end{pmatrix} \quad (1)$$

where $a = [(1-2\epsilon)^{1/2}-1]/2$, $b = [(1-2\epsilon)^{1/2}+1]/2$ and ϵ , $0 \leq \epsilon \leq 1/2$, is called coupling constant, since $\epsilon=0$ and $\epsilon=1/2$ correspond to decoupling and strong coupling of a ring with leads, respectively. Scatterers are described by a transfer or t -matrix. Since we consider a one-dimensional system, the t -matrix is given by

$$\underline{t} = \begin{pmatrix} 1/t^* & -r^*/t^* \\ -r/t & 1/t \end{pmatrix} \quad (2)$$

Here $t = T_s^{1/2} e^{i\phi}$ is the transmission amplitude of the scatter, T_s the transmission probability and ϕ the phase change in the transmitted

wave. The reflection amplitude of the scatter is given by $r = R_S^{1/2} e^{i\phi} e^{-i\pi/2}$. Generally t and r are functions of electron energy, magnetic field and disorder of the metal. Following the formalism developed by Buttiker et al.,¹¹ the total transmission coefficient is obtained as a function of magnetic flux, Φ , T_S and phases ϕ_1 and ϕ_2 for the two branches of the ring. We find that the total transmission coefficient T is given by $T = |a_2'|^2$, where a_2' is

$$a_2' = \frac{2i\epsilon T_S^{1/2} [(\sin\phi_1 + \sin\phi_2 + 2R_S^{1/2}) \cos\pi(\Phi/\Phi_0) + i(\sin\phi_1 - \sin\phi_2) \sin\pi(\Phi/\Phi_0)]}{2b^2 T_S \cos 2\pi(\Phi/\Phi_0) + C} \quad (3)$$

where

$$C = 2a^2 \cos(\phi_1 - \phi_2) - 2R_S(b^2 - 2a^2) - (1 - 2\epsilon) \exp[i(\phi_1 + \phi_2)] - \exp[-i(\phi_1 + \phi_2)] \\ - 2iaR_S^{1/2} \{(1 - 2\epsilon)^{1/2} [\exp(i\phi_1) + \exp(i\phi_2)] + \exp(-i\phi_1) + \exp(-i\phi_2)\}$$

Φ is the magnetic flux through the hole and $\Phi_0 = hc/e$ is the flux quantum. We immediately see from Eq. (3) that the transmission coefficient T is a periodic function of flux with period of the flux quantum hc/e . These results are in agreement with those of Refs. 10 and 12. Eq. (3) can be simplified a lot if we approach the weak scattering limit where $T_S = 1$ for the two scatterers in the branches of the ring, while the phase changes in the transmitted waves in the two scatterers are ϕ_1 and ϕ_2 respectively. In this limit the total transmission coefficient is given by

$$T = |a_2'|^2$$

$$= \frac{\epsilon^2 [\sin^2 \phi_1 + \sin^2 \phi_2 + 2 \sin \phi_1 \sin \phi_2 \cos 2\pi(\phi/\phi_0)]}{[b^2 \cos^2 \pi(\phi/\phi_0) - (1-\epsilon) \cos(\phi_1 + \phi_2) + a^2 \cos(\phi_1 - \phi_2)]^2 + \epsilon^2 \sin^2(\phi_1 + \phi_2)} \quad (4)$$

For $\phi_1 = \phi_2$, Eq. (4) agrees with the Eq. (4.25) of Ref. 11, which has been studied very carefully and always shows a periodicity of full flux. We see, from Eq. (4), that for a single configuration of the disordered ring in the presence of magnetic field, the transmission coefficient T will always be a periodic function of full flux at zero temperature. However, if we average over the disorder Eq. (4) we might obtain the half-flux oscillation as was speculated.^{11,13} Note that in the weak scattering limit $T_s = 1$ and only ϕ_1 and ϕ_2 are randomly distributed with a rectangular probability distribution between 0 and 2π . In the weak-scattering limit, this is shown to be true¹⁵ for the one-dimensional Anderson model with diagonal disorder. Therefore, in this regime, averaging over the phases ϕ_1 and ϕ_2 must be taken, and the macroscopic properties of the sample are the ensemble averaged quantities. We use uniform phase distribution. Hence, the geometric average of the total transmission coefficient is given by

$$\langle T \rangle_g = e^{\langle \ln T \rangle} \quad , \quad (5a)$$

where

$$\langle \ln T \rangle = \frac{1}{2\pi^2} \int_0^{2\pi} d\phi_1 \int_0^{2\pi} d\phi_2 \ln T(T_s, \phi_1, \phi_2, \epsilon, \phi) \quad (5b)$$

We also calculate the arithmetic average of T which is a direct average of T in Eq. (5b). T , in Eq. (5b), can be taken either from Eq. (4) or Eq. (3). For $T_s = 1$, Eq. (5b) together with Eq. (4), indeed shows that such an average over disorder will change the period to $hc/2e$. This can be seen clearly from the relation

$$T(T_s=1, \phi_1, \phi_2, \epsilon, \phi + \phi_0/2) = T(T_s=1, \phi_1 + \pi, \phi_2, \epsilon, \phi) \quad (6a)$$

hence,

$$\langle T \rangle |_{\phi + \phi_0/2} = \langle T \rangle |_{\phi} \quad (6b)$$

This is correct for the geometric as well as the arithmetic average of the transmission coefficient T for $T_s=1$. The geometric average $\langle T \rangle_g$ of T for different coupling constants ϵ is plotted in Fig. 1. The striking feature is that $\langle T \rangle_g / \epsilon^2$ is extremely insensitive to changes of the coupling constant. From Fig. 1, we clearly see that T is a periodic function of half flux quantum $\phi_0/2$. As a comparison, we plot in Fig. 2 the arithmetic average $\langle T \rangle_a$ of the total transmission coefficient T as a function of the flux through the hole of the ring. In this case too, the period of oscillation of $\langle T \rangle_a$ is half-flux quantum but $\langle T \rangle_a / \epsilon^2$ does depend on the coupling constant, ϵ .

Similar oscillations have been seen in the work of Carini et al.⁹ for the participation ratio. Our results suggest that the ensemble-average picture presented in Ref. 9 and the perturbation theory of AAS¹ and Bergmann⁸ are not so different from that expressed in the transfer

matrix picture, provided an ensemble average over disorder is taken. It is very interesting that if we average total transmission coefficient T over the phases ϕ_1 and ϕ_2 [Eq.(3)] when $T_S < 1$, we find that $\langle T \rangle_g$ and $\langle T \rangle_a$ are not periodic functions of half flux anymore, but of full flux. This is clearly shown in Figs. 3a and 3b, where $\langle T \rangle_g/\epsilon^2$ and $\langle T \rangle_a/\epsilon^2$ are, respectively, plotted as a function of magnetic flux through the hole of the ring for $\epsilon = 1/2$ and different values of T_S .

By carefully examining Figs. 3a and 3b, we notice that the transmission coefficient has a full-flux oscillation, but there is also an appreciable component of a half flux. The oscillations of the transmission coefficient in Fig. 3b are very similar to those seen in Fig. 1(c) of Ref. 9 for small size rings, for the participation ratio. They interpreted their numerical results as half-flux oscillations because their time-reversal-symmetry arguments will persist for any size system. Most astonishing is our result that even after ensemble averaging for $T_S < 1$, the transmission coefficient is periodic in hc/e . Although the results are not periodic with period $hc/2e$, there is also a significant decrease in the transmission coefficient for half-integer values of ϕ/ϕ_0 [see Fig. 3(b)]. The general philosophy in the field is that ensemble averaging kills the hc/e . We believe that this statement might indeed lack precision; presumably, it depends on the ensemble average being considered. Expressed otherwise, ensembles which are not "wild" enough might not be sufficient to lead to the self-averaging of the hc/e component. The important question then is,

"what is a physically relevant ensemble, i.e., which ensemble incorporates the variations from member to member which we would expect in a real system?" In this work, as an ensemble average, we take that one in which the distribution of phases is uniform. We know that this is true for the weak-scattering limit,¹⁵ but it is possible that the distribution is no longer uniform for strong disorder, and this might be the reason for differences between our results and those of Ref. 9. Note that as T_s decreases from the value one, which corresponds to the weak-scattering limit, the period of oscillation of $\langle T \rangle_g$ and $\langle T \rangle_a$ gradually shifts towards the full flux quantum. So for the strong scattering case, i.e., $T_s \ll 1$, the hc/e period would become dominant. This is simply related to the fact that the $hc/2e$ period oscillation involves backscattering interference⁸ in which electrons effectively circle around the ring twice. Therefore, for the strong-scattering case, electron waves would be greatly attenuated and phase-coherence around the whole ring would almost be lost, and the contribution with the hc/e period would be observed. It can be argued that, as the magnetic field is increased, the transmission amplitude T_s of the scatterer will be decreased, and therefore, $\langle T \rangle_g$ or $\langle T \rangle_a$ will show full flux quantum oscillations in agreement with experiments⁷ which study the magnetic field dependence of T . Very recently, Stone and Imry¹⁶ have argued that increasing temperature will cause single ring self-average; the flux periodicity of the magnetoresistance oscillations become $hc/2e$. Of course, at zero temperature with no self-average, the oscillations are of the hc/e type.

Conclusions

To summarize, we have shown that the transmission coefficient of a normal metal ring with contacts will oscillate as a function of the magnetic flux with a period of half-flux quantum in the weak scattering case. For the strong scattering case, full-flux quantum oscillations are dominant. All of these results are correct for zero temperature. To make a comparison with the experimental results^{6,7} we have to define the important characteristic lengths and discuss their dependence on temperature, disorder and magnetic field. One is the electron phase coherence length, L_c , which is the distance that an electron travels before randomly changing its wave-function phase. L_c is, roughly speaking, the mean free path which, for a typical metal⁷, is of order of 10-100 Angstroms and independent of temperature. The inelastic diffusion length is $L_{in} = (D\tau_{in})^{1/2}$, where D is the diffusion constant (assumed to be temperature independent) and τ_{in} is the mean time between inelastic collisions. It is expected that τ_{in} is inversely proportional to the temperature. L_{in} can be larger than 1 μm at low temperatures (1 $\mu\text{m} = 10^4$ Angstrom)⁷. The localization length, l_c , has to be of the order of L_{in} if one wants to see these electron interference effects. Finally the magnetic length is $L_H \sim (hc/eWH)$, where H is the applied magnetic field and W the width of the sample. The ratios of these lengths to the sample length, L , govern the size (or the presence) of the oscillations. The condition for observing the

Aharonov-Bohm effect with half-flux quantum in disordered rings is that $L_{in} \sim l_c \sim L_H \geq L \gg l$, where L is the perimeter of the ring. This has to be distinguished from Aharonov-Bohm resistance oscillations in very pure single-crystal with a long mean free path, $l \gg L$, and with a period of hc/e . In the disordered ring, the oscillations with half-flux will gradually give way to hc/e oscillations as we increase either the magnetic field or the disorder. In these two cases l_c or L_H will decrease and phase coherence around the whole perimeter of ring L will be destroyed and with it the $hc/2e$ oscillation, too. This picture agrees with the experimental results.⁷ Finally, by increasing the temperature, L_{in} decreases and eventually will become smaller than $L/2$. This phase-incoherence introduced by increasing the temperature, will destroy both the periods of oscillations of the magnetoresistance.

Acknowledgments

We acknowledge helpful discussions with E. N. Economou and A. D. Stone. Ames Laboratory is operated for the U.S. Department of Energy by Iowa State University under Contract No. W-7405-Eng-82.

References

1. B. L. Al'tshuler, A. G. Aronov, and B. Z. Spivak, Pis'ma Zh. Eksp. Teor. Fiz. 33, 101 (1981) [JETP Lett. 33, 94 (1981)].
2. D. Yu. Sharvin and Yu. V. Sharvin, Pis'ma Zh. Eksp. Teor. Fiz.

- 34, 285(1981) [JETP Lett. 34, 272 (1981)].
3. B. L. Al'tshuler, A. G. Aronov, B. Z. Spivak, D. Yu. Sharvin, and Yu. V. Sharvin, Pis'ma Zh. Eksp. Teor. Fiz. 35, 476 (1982) [JETP Lett. 35, 588 (1982)].
 4. M. Gijs, C. Van Haesendonck, and Y. Bruynseraede, Phys. Rev. Lett. 52, 2069 (1984).
 5. B. Pannetier, J. Chaussy, R. Rammal, and P. Gandit, Phys. Rev. Lett. 53, 718 (1984).
 6. R. A. Webb, S. Washburn, C. P. Umbach, and R. B. Laibowitz, Phys. Rev. Lett. 54, 2696 (1985); Phys. Rev. B 32, 4789 (1985).
 7. V. Chandrasekhar, M. J. Rooks, S. Wind, and D. E. Prober, Phys. Rev. Lett. 55, 1610 (1985).
 8. G. Bergmann, Phys. Rev. B 28, 2914 (1983). In this work the back-scattering contribution to the conductivity of the two time reversed paths which return to the origin is considered. This leads to an enhanced contribution to the conductivity at $hc/2e$.
 9. J. P. Carini, K. A. Muttalib, and S. R. Nagel, Phys. Rev. Lett. 53, 102 (1984); D. A. Browne, J. P. Carini, K. A. Muttalib, and S. R. Nagel, Phys. Rev. B 30, 6798 (1984).
 10. Y. Gefen, Y. Imry, and M. Ya. Azbel, Phys. Rev. Lett. 52, 129 (1984); Surf. Sci. 142, 203 (1984).
 11. M. Buttiker, Y. Imry, and R. Landauer, Phys. Lett. 96A, 365 (1983); M. Buttiker, Y. Imry, and M. Ya. Azbel, Phys. Rev. A 30, 1982 (1984).
 12. M. Buttiker, Y. Imry, R. Landauer, and S. Pinhas, Phys. Rev. B

- 31, 6207 (1985).
13. Y. Gefen (unpublished).
 14. A. D. Stone, Phys. Rev. Lett. 54, 2692 (1985); P. A. Lee and A. D. Stone, Phys. Rev. Lett. 55, 1622 (1985).
 15. A. D. Stone, D. C. Allan, and J. D. Joannopoulos, Phys. Rev. B 27, 836(1983); C. J. Lambert and M. F. Thorpe, Phys. Rev. B 26, 4742 (1983); M. Ya. Azbel and M. Rubinstein, Phys. Rev. Lett. 51, 836 (1983).
 16. A. D. Stone and Y. Imry, Phys. Rev. Lett. 56, 189 (1986)

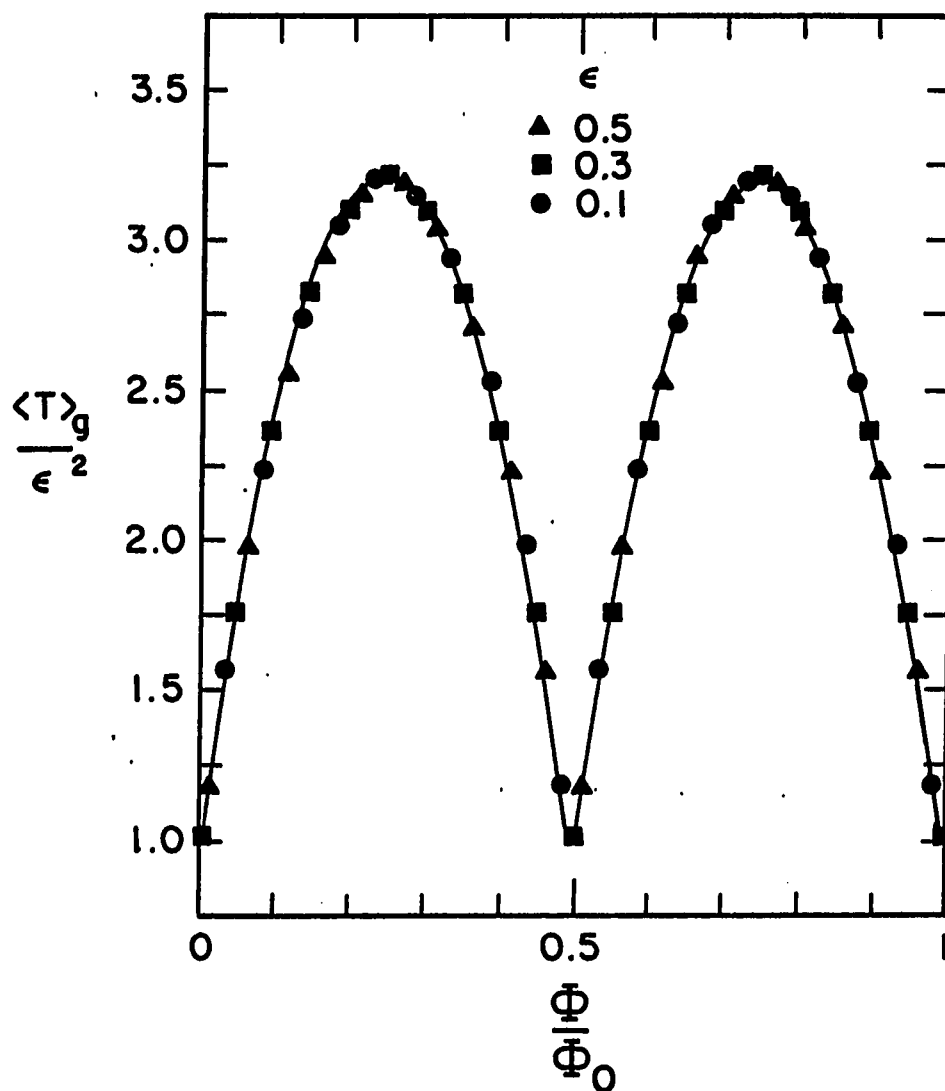


Fig. 1. $\Phi_0/2$ oscillations of the geometric average of the total transmission coefficient for different degrees of coupling for weak scattering $T_S=1$

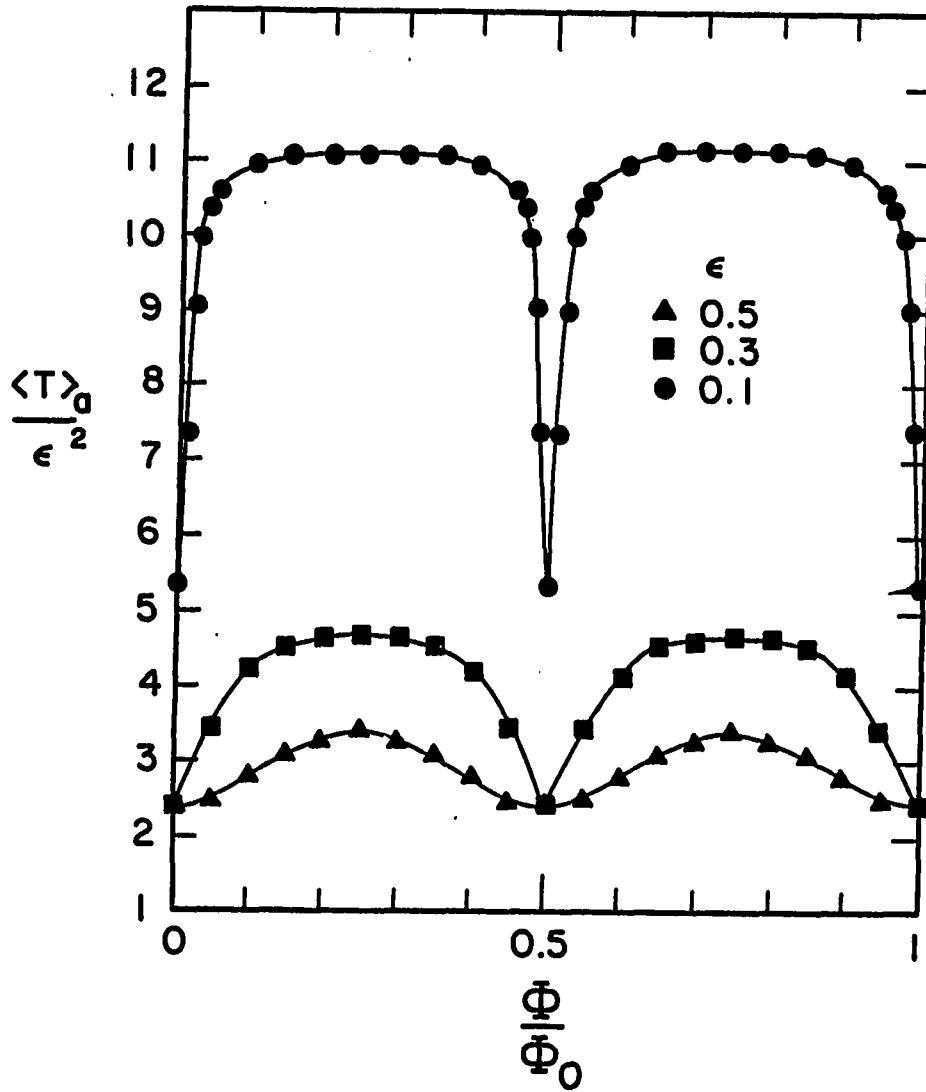


Fig. 2. $\Phi_0/2$ oscillations of the arithmetic average of the total transmission coefficient for different degrees of coupling for weak scattering $T_S=1$

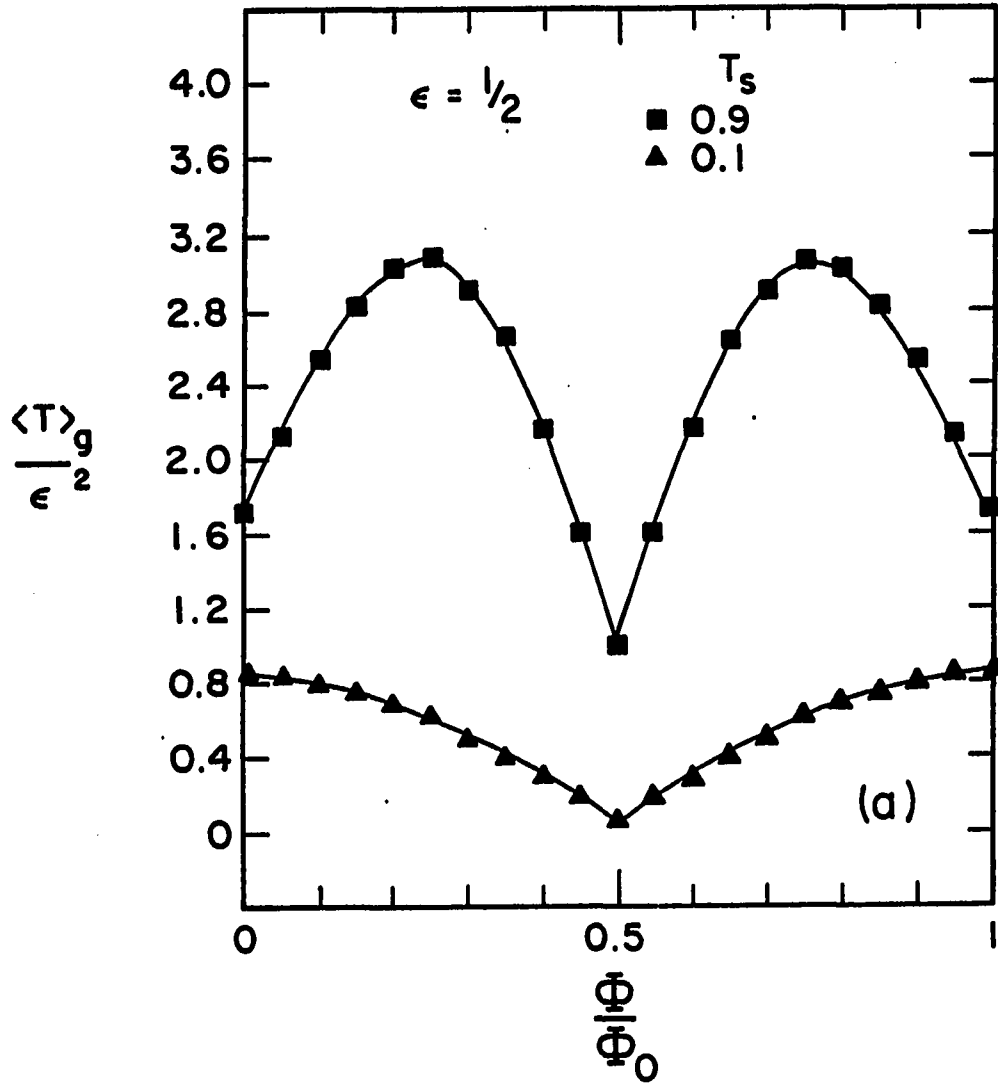


Fig. 3a. Geometric average $\langle T \rangle_g$ of the total transmission coefficient as a function of magnetic flux through hole for different T_s for $\epsilon = 1/2$.

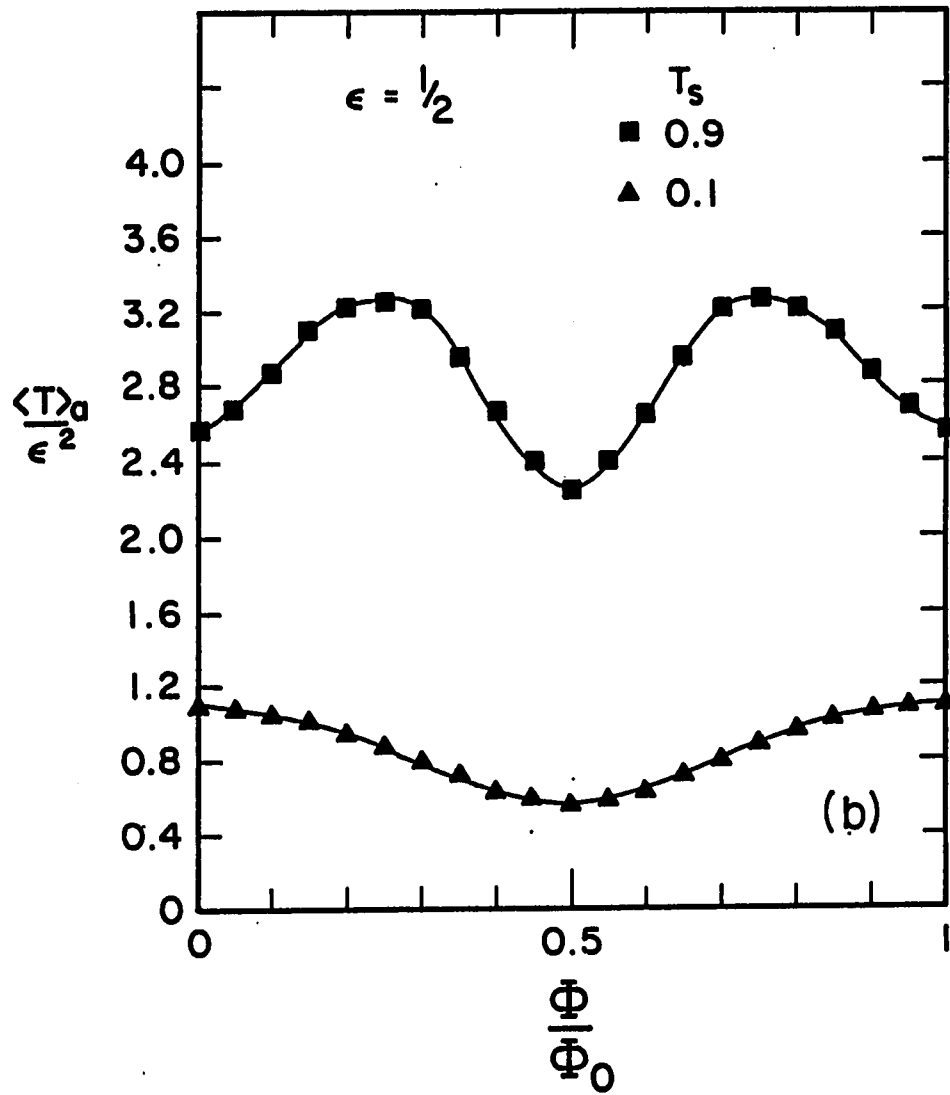


Fig. 3b. Arithmetic average $\langle T \rangle_a$ of the total transmission coefficient as a function of magnetic flux through hole for different T_s for $\epsilon = 1/2$

PART II.
HALF-FLUX-QUANTUM MAGNETORESISTANCE OSCILLATIONS
IN DISORDERED METAL RINGS

Abstract

The behavior of the magnetoresistance of single and arrays of disordered metal rings is investigated. The average localization length, L_c , which is related with the conductance, is found to oscillate with strong half-flux quantum harmonic at low magnetic field. The ratio of the amplitude of the full-flux oscillations versus the half-flux oscillation is shown to decrease with the number of rings. All numerical results follow a universal law where the amplitude of oscillations of L_c is found to be proportional to the square of the ratio of L_c to the perimeter of the ring. At high magnetic fields, full-flux oscillations are observed.

Introduction

The half-flux-quantum oscillations of magnetoresistance of disordered metal rings and cylinders, predicted by Al'tshuler, Aronov, and Spivak (AAS),¹ have been observed experimentally on disordered cylinders and arrays of rings by several groups.²⁻⁵ Experiments on single rings, on the other hand, showed complicated features. Full-flux quantum oscillation was observed by Webb et al.⁶ on small gold rings. Later, Chandrasekhar⁷ et al. observed $h/2e$ oscillations at low field and h/e oscillations at higher field on single aluminum and silver rings. Very recently both h/e and the AAS $h/2e$ oscillations were measured⁸ in samples consisting of N rings connected in series.

Clear evidence was found that averaging leads to a $N^{-1/2}$ dependence of the amplitude of the h/e oscillation while the amplitude of the $h/2e$ oscillations is independent of the number of rings.

The AAS effect results from the quantum corrections to conductance due to backscattering interference.⁹ Theoretical works based on calculating the transmission coefficient in one-dimensional metal rings,¹⁰⁻¹² however, showed that the fundamental period of oscillation at zero temperature is full-flux quantum and that higher harmonics become dominant only at special conditions. The very important difference between the two theories is that the former employed the ensemble average. Carini, Muttalib, and Nagel¹³ also showed that the existence of degeneracies and time-reversal invariance of the Hamiltonian after ensemble average could lead to $h/2e$ oscillation. It has recently been shown¹⁴ that for a symmetric normal metal ring, averaging of the transmission coefficient T over disorder gives oscillations with a period of $h/2e$. As the elastic scattering gets stronger, the periodicity of the magnetoresistance oscillations becomes h/e . Numerical simulation of transmission matrix method by Stone and Imry¹⁵ also showed $h/2e$ oscillation when ensemble averaging is performed. Existence of uncorrelated regions and thermal smearing¹⁵ is an important source of self-averaging. Complications due to the aperiodic fluctuations added to the magnetoresistance also exist in small samples.¹⁶

Results and Discussion

In this paper, we present the results of a detailed numerical simulation on a single small ring and rings connected in series. The disorder, width, magnetic field, and length dependence of the transmission coefficient, which is related to L_c , for the rings will be presented.

We simulate a small rectangular ring by a two dimensional strip described by a nearest-neighbor tight-binding Hamiltonian

$$H = \sum_{lm} \epsilon_{lm} |lm\rangle\langle lm| + \sum_{l'm'lm} V_{lm,l'm'} |lm\rangle\langle l'm'|. \quad (1)$$

$|lm\rangle$ denotes the site corresponding to the respective x,y coordinate. The strip boundary geometry can be set by proper choice of the site energies ϵ_{lm} and the hopping matrix elements $V_{lm,l'm'}$. ϵ_{lm} are generally taken as independent random variables uniformly distributed between $\pm W/2$ in the disordered region of the ring. As a result of our method of calculation outside the ring area, ϵ_{lm} are set to very large values (infinite potential barriers) so that the electrons will be moving only inside the ring area. A uniform magnetic field, normal to the ring, introducing a phase to the hopping matrix element can be taken into consideration via Peierls substitution¹⁷

$$V_{lm,l'm'} = \begin{cases} 1 & \text{if } m=m' \text{ and } l'=l\pm 1 \\ e^{\pm i\alpha l} & \text{if } l=l' \text{ and } m'=m\pm 1, \end{cases} \quad (2)$$

where α is the number of flux quanta per unit cell $\alpha = eB/h$ and the lattice constant is taken to be 1.

We use the recursive Green's function method to calculate¹⁷ the localization length. Free boundary conditions are used in the transverse direction (y direction). The imaginary part of the energy is taken to be 2×10^{-4} in unit of V . Since the Aharonov-Bohm effect depends only on the topology, following Stone,^{15,16} we make a small hole in the middle of the strip but with much larger magnetic field in the hole than in the annulus. This way we can save on computer time and achieve a good aspect ratio (the ratio of the flux through the hole to that through the annulus), which is important in order to observe $h/2e$ oscillations. We also attach on one end a semi-infinite disordered "lead" to achieve stable values for the localization length. The geometry of the ring is the following: L is the length of the long side of the rectangular ring, M is the width of the strip, and MW is the width of the ring. In our numerical studies, we always calculate the localization length which is related to the conductance by the Landauer's formula¹²

$$G = (2e^2/h) / (e^{2L/L_c} - 1) \quad (3)$$

where L is the perimeter of the loop and L_c is the localization length. Throughout this paper formula (3) will be adopted.

We organize our results as follows:

(1) Single ring without average over disorder.—Single ring at zero temperature does not have a self-average property.¹⁵ For $L_c > L$ we expect an oscillation of fundamental period h/e with a smaller $h/2e$ component. This is indeed what we observed in our simulation. For strong disorder, as can be seen in Fig. 1(a), an h/e oscillation is observed for all the widths we studied. However, for some specific configuration of weak disorder, where $L_c \gg L$, a very good $h/2e$ oscillation was present as seen in Fig. 1(b). These accidental $h/2e$ oscillations are very sensitive to disorder configurations and energy and gradually transform to h/e oscillation in higher magnetic field. In most of cases we studied, the h/e component dominates, in agreement with results of the transmission coefficient for a normal-metal ring with contacts.^{10-12,14}

(2) Single ring with ensemble average.—In all the cases we studied, averaging over different configurations of disorder gives an $h/2e$ oscillation in the localization length, and, through Eq. (3), in the conductance of a single ring. This is clearly seen in Fig. 1(c) where L_c versus the flux through the ring is plotted. Note that the $h/2e$ oscillation is the dominant one. Therefore, the ensemble averaging brings the period $h/2e$. The convergence, however, can be very slow when $L_c \gg L$. Note also in Fig. 1(c) that for strong magnetic fields, the $h/2e$ oscillation is not too dominant and the h/e oscillation starts to appear. For even strong magnetic fields, as one

can see from the insert of Fig. 1(c), there is even more structure within a full-flux. This feature has to be investigated further.

(3) Series-connected rings.— $h/2e$ oscillations are seen again in this case, too, when a large number of rings are connected in series. In Fig. 1(d) we show results for $N = 50$ rings in series of width $MW=4$ and disorder $W = 2.0$ averaged over 100 different configurations of disorder; a perfect $h/2e$ oscillations is observed. Again in this case the dominant oscillation is the $h/2e$.

(4) h/e versus $h/2e$ component.— Recently detailed experiments⁸ have been performed to test the stochastic averaging of the h/e oscillations. In the experiment⁸ it was clearly shown that the h/e and the $h/2e$ oscillations coexist when the ring number is small. At constant temperature, the h/e component was found to decrease with square root of the number of loops N , while the amplitude of the $h/2e$ component was independent of the number of rings. We have performed systematic simulations to check the experimental results and predict possible new behaviors. We have used 100 configurations to represent the finite temperature.¹⁵ Then we added single rings one by one in series. To extract the h/e and $h/2e$ component from the total conductance (localization length L_c) oscillation, we used an approximation which neglects higher harmonics and assumed the total conductance consisted of only the h/e component and $h/2e$ component, i.e.,

$$G(\phi/\phi_0) = G_0 + 0.5A_1 \cos(\phi/\phi_0) + 0.5A_2(2\phi/\phi_0) \quad (4)$$

where $\Phi_0 = h/e$. As can be seen from Fig. 1, the curves are relatively smooth and so the approximation in Eq. (4) is fine. Therefore, we have that $A_1 = |G(1/2) - G(0)|$ and $A_2 = |G(0) - G(1/4) + G(1/2) - G(3/4)|/2$. In Fig. 2 we plot the relative values of A_1 with respect to A_2 as a function of the ring number for two different geometries. We see that the h/e component decreases inversely proportional to the number of rings relatively to the $h/2e$ component. This seems to disagree with the experimental results⁸ which claim a $1/N^{1/2}$ decrease of the h/e component. This discrepancy might be a result of the different way of extracting the two components in our simulations and in the experiments.

(5) Amplitude of oscillation.— The size of the interference effects depends on the range of coherence of the diffusion electrons and is limited by other phase breaking processes. Among the most important are inelastic scattering and magnetic scattering. In our model, the relevant physical lengths are the perimeter of the loop, the localization length, and the magnetic field length, $L_B \sim h/e(MW)B$. At low magnetic fields B , it is the ratio of L_C to L which determines the size of the oscillation. To test this idea, we numerically calculate the conductance of rings of different perimeters, different widths, and different strengths of disorder W . The results are shown in Fig. 3, where the amplitude of the oscillation for small fields B is plotted as a function of L_C/L . We indeed see that all the data of the different cases we examined scale in a universal curve. In particular, we have

that the magnitude of the oscillation of the localization length, L_c , is $\Delta L_c/L = 0.067 (L_c/L)^2$, for all the widths, perimeters, L , and disorder, W . Notice that as L_c/L increases, the magnitude of the conductance oscillations also increases. Our results suggest that it is possible to have conductance fluctuations¹⁸ of values higher than e^2/h . In particular, for a single-ring geometry and $L_c/L=35$, we obtain $\Delta G = 10.4 e^2/h$ as a conductance fluctuation. Meanwhile, for a series of rings and $L_c/L = 10$, we obtain $\Delta G = 8.3e^2/h$. Stone and Imry¹⁵ have only calculated a particular case of L_c/L and their results are in qualitative agreement with ours. In particular, from the top of Fig. 2 in Ref. 15, we have that $G_{\max} = 3.2 e^2/h$ and the magnitude of the $h/2e$ conductance oscillations is given by $\Delta G = 0.05e^2/h$. From the value of G and Eq. (3), we obtain $L_c/L = 4.1$ and from the ΔG value we have that $\Delta L_c/L = 0.05$ which is lower than our estimates. This difference is due to the fact that Stone and Imry¹⁵ used a single ring and averaged over disorder. In Fig. 3 we plotted the data for fifty rings connected in series and then averaged over disorder. The single ring data also follows a universal law, the only difference is that $\Delta L_c/L = 0.0025 (L_c/L)^2$ instead of $\Delta L_c/L = 0.067(L_c/L)^2$. These laws will break down when $\Delta L_c/L$ is of order 1. We want to mention that the data shown in Fig. 3 are the overall amplitude oscillations of L_c for small field B . For $L_c < L$, the $h/2e$ component is the dominant oscillation. For $L_c > L$, we might have a $h/2e$ oscillation. Sometimes a h/e oscillation is also present.

Conclusions

In conclusion, our work demonstrates unambiguously that single rings, when averaged over disorder, do exhibit quantum interference effects, with a flux period $h/2e$ at low fields and with a flux period of h/e clearly visible at higher fields (see, for example, Fig. 1(c)). This behavior has been suggested in Refs. 10-12, but it was only recently shown to be correct by Refs. 14 and 18 for the transmission coefficient. This picture agrees with the experimental results. Our numerical results provide a universal law for the strength of the oscillation of the magnetoresistance. The oscillation strength only depends on the ratio of the relevant lengths: the ring perimeter, and the localization length. In particular, when $L_c \leq L$, the magnetoresistance is $h/2e$ periodic, but, as L_c increases, the h/e harmonic dominates and finally, when $L_c \geq L$, the $h/2e$ harmonic might disappear completely. At the other extreme, when $L_c < L$, the $h/2e$ periodicity persists, but the oscillation amplitude decreases with respect to the background value. It will be very interesting to check experimentally this universal behavior. The above phenomena have been observed for rings of width $MW=1$ as well as for rings of finite width. For the finite width rings, the $h/2e$ oscillation is seen when the mean free path, l , which is different than L_c , becomes smaller than L . Details of this behavior will be published elsewhere. Finally, by increasing the temperature, the inelastic mean free length decreases and eventually will become smaller than L . This phase incoherence

introduced by increasing the temperature will destroy both periods of the magnetoresistance.

Acknowledgments

We acknowledge helpful discussions with G. S. Grest and S. R. Nagel. Ames Laboratory is operated for the U.S Department of Energy by Iowa State University under Contract No. W-7405-Eng-82.

References

1. B. L. Al'tshuler, A. G. Aronov, and B. Z. Spivak, Pis'ma Zh. Eksp. Teor. Fiz. 33, 101 (1981) [JETP Lett. 33, 94 (1981)].
2. D. Yu. Sharvin and Yu. V. Sharvin, Pis'ma Zh. Eksp. Teor. Fiz. 34, 285(1981) [JETP Lett. 34, 272 (1981)]; B. L. Al'tshuler, A. G. Aronov, B. Z. Spivak, D. Yu. Sharvin, and Yu. V. Sharvin, Pis'ma Zh. Eksp. Teor. Fiz. 35, 588 (1982)).
3. G. J. Dolan, J. C. Licini, and D. J. Bishop, Phys. Rev. Lett. 56, 1493 (1986).
4. M. Gijs, C. Van Haesendonck, and Y. Bruynseraede, Phys. Rev. Lett. 52, 2069 (1984).
5. B. Pannetier, J. Chaussy, R. Rammal, and P. Gandit, Phys. Rev. Lett. 53, 718 (1984).
6. R. A. Webb, S. Washburn, C. P. Umbach, and R. B. Laibowitz, Phys. Rev. Lett. 54, 2696 (1985); Phys. Rev. B 32, 4789 (1985).

7. V. Chandrasekhar, M. J. Rooks, S. Wind, and D. E. Prober, Phys. Rev. Lett. 55, 1610 (1985).
8. C. P. Umbach, C. Van Haesendonck, R. B. Leibowitz, S. Washburn, and R. A. Webb, Phys. Rev. Lett. 56, 386 (1986).
9. G. Bergmann, Phys. Rev. B 28, 2914 (1983). In this work, the backscattering contribution to the conductivity of the two time-reversed paths which return to the origin is considered. This leads to an enhanced contribution to the conductivity at $h/2e$.
10. Y. Gefen, Y. Imry, and M. Ya. Azbel, Phys. Rev. Lett. 52, 129 (1984); Surf. Sci. 142, 203 (1984).
11. M. Buttiker, Y. Imry, and R. Landauer, Phys. Lett. 96A, 365 (1983); M. Buttiker, Y. Imry, and M. Ya. A'zbel, Phys. Rev. B 30, 1982 (1984).
12. M. Buttiker, Y. Imry, R. Landauer, and S. Pinhas, Phys. Rev. B 31, 6207 (1985).
13. J. P. Carini, K. A. Muttalib, and S. R. Nagel, Phys. Rev. Lett. 53, 102 (1984); D. A. Browne, J. P. Carini, K. A. Muttalib, and S. B. Nagel, Phys. Rev. B 30, 6798 (1984).
14. Qiming Li and C. M. Soukoulis, Phys. Rev. B 33, 7318 (1986).
15. A. D. Stone and Y. Imry, Phys. Rev. Lett. 56, 189 (1986).
16. A. D. Stone, Phys. Rev. Lett. 54, 2692 (1985); P. A. Lee and A.

- D. Stone, Phys. Rev. Lett. 55, 1622 (1985).
17. L. Schweitzer, B. Kramer, and A. Mackinnon, J. Phys. C 17, 4111 (1984); A. Mckinnon, Z. Phys. B 59, 385 (1985).
18. M. Murat, Y. Gefen, and Y. Imry, Phys. Rev. B 34, 659(1986).

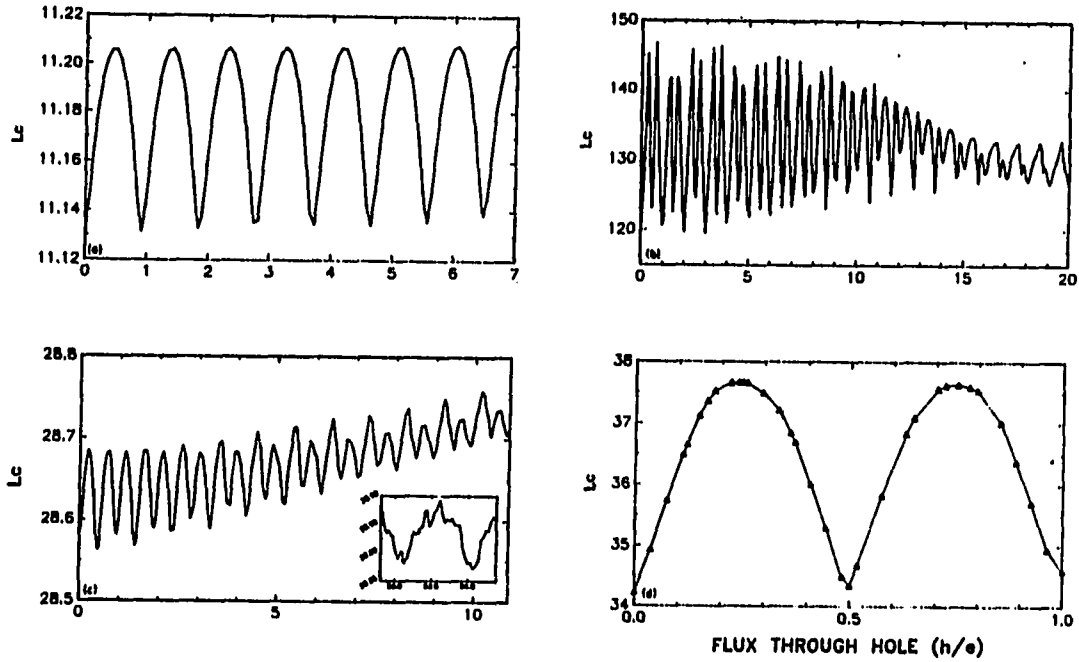


Fig. 1. Quantum oscillations of the localization length L_c , which is related with the conductance G through Eq. (3), for the following cases: (a) A single ring with disorder $W=4.0$. No average over disorder is taken. The h/e oscillation is clearly observed. (b) A single ring with disorder $W=1.2$. No average over disorder is taken. The $h/2e$ oscillation is observed at small magnetic fields B and at high B gradually changes to h/e . (c) a single ring with disorder $W=2.0$. Average over 1000 disorder configurations is taken. Insert: the behavior of L_c for very strong magnetic fields. (d) A series of 50 rings with disorder $W=2.0$. Average over 100 disorder configurations is taken. In all the cases the width and length of the ring are $MW=4$ and $L=30$, respectively. The aspect ratio is 7

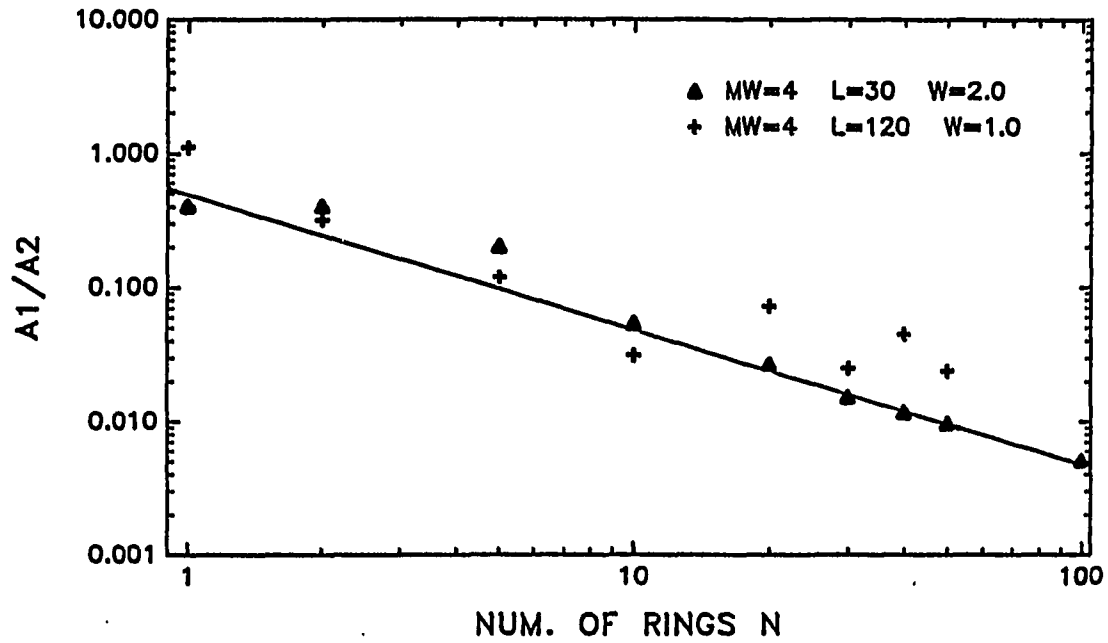


Fig. 2. The ratio A_1/A_2 versus the number of rings N on a log-log plot for different values of lengths L and disorder W . A_1 and A_2 are the amplitudes for the h/e and $h/2e$ oscillations of the conductance, respectively.

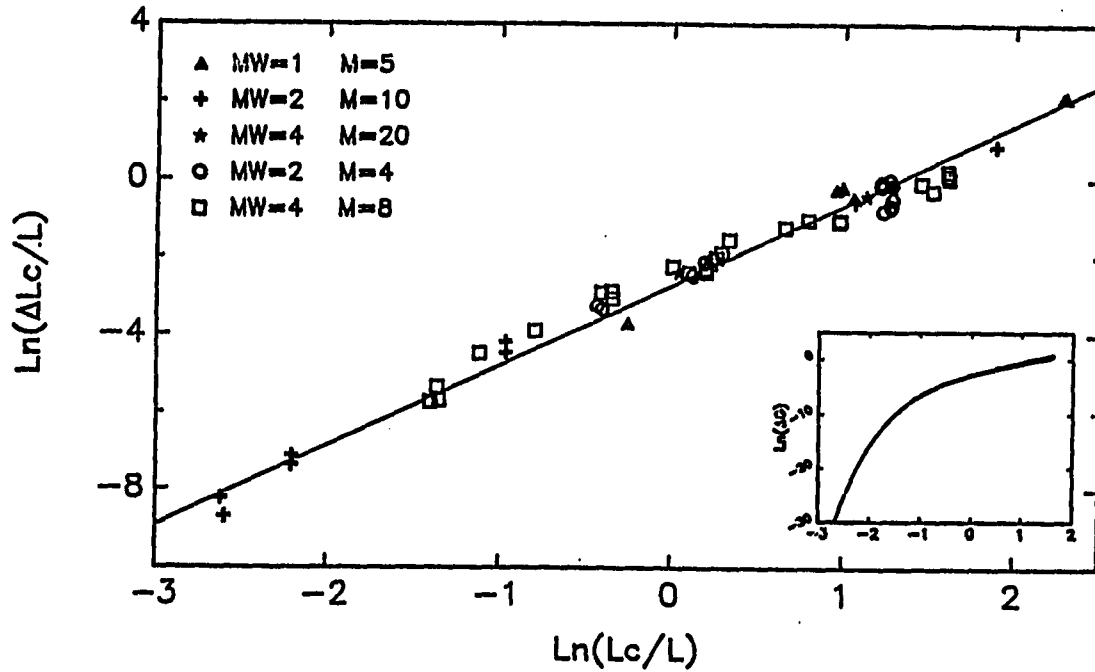


Fig. 3. Magnitude $\Delta(L_c/L)$ of the oscillation of localization length L_c , versus L_c/L for different widths, lengths, disorder. The number of rings ranges from 40 to 100. Insert: the magnitude of the conductance oscillation plotted versus L_c/L

PART III.
METAL-INSULATOR TRANSITION
IN RANDOM SUPERCONDUCTING NETWORKS

Abstract

The nature of the eigenstates and the effects on the superconducting-to-normal phase boundary in a two-dimensional random superconducting network is examined by finite-size scaling transfer matrix calculations within the mean-field Ginzburg-Landau theory of second order phase transitions. Results for both site and bond diluted square lattices are presented and a rich structure in the mobility edge trajectory is obtained. The critical exponent for the slope of the critical field on $(p-p_c)$ is calculated and compared with previous estimates.

Introduction

In recent years, considerable attention has been devoted to the study of flux quantization effects, which have been theoretically predicted¹⁻³ and experimentally observed,⁴⁻⁷ in arrays of superconducting honeycomb,⁴ square,⁵ self-similar,⁶ and quasicrystal⁷ networks. The main feature of this quantization effect is the oscillation of the superconducting transition temperature $T_c(H)$ as a function of the external magnetic field H . For example, in a perfect periodic network, $T_c(H)$ exhibits singularities at rational values of the reduced flux Φ/Φ_0 , where $\Phi = HL^2$ is the magnetic flux through the unit cell of the superconducting network and $\Phi_0 = hc/2e = 2.07 \times 10^{-7}$ G cm² is the superconducting flux quantum. It was recognized⁵ several

years ago that such a superconducting network is an ideal experimental system for studying the effects of frustration in a well-characterized system. In this system, the reduced flux is the frustration parameter and can be changed continuously. The mean-field Ginzburg-Landau theory of second-order phase transitions, as developed by de Gennes¹ and Alexander,² provides a very accurate description of these phenomena. Most of the research effort so far has been concentrated on understanding the superconducting-to-normal phase boundary in various periodic networks. Only very recently some attempts have been made to experimentally^{8,9} and theoretically^{9,10} calculate the superconducting phase boundary for random superconducting networks. The expected dimensionality crossover between the homogeneous and fractal regimes was not observed⁸ in the random square lattice bond percolating networks. Furthermore, the interesting problem of the superconducting phase below T_c has not been addressed¹¹ beyond the mean-field approximation.

Results and Discussion

In this Rapid Communication, we study the superconducting-to-normal (S-N) phase boundary for a random percolating superconducting network. The networks could be either site or bond diluted. As expected, the structure of the phase boundary curve $T_c(H)$ is washed out due to the randomness of the percolation networks. By examining the nature of the eigenstates for different values of the concentration of

the sites or the bonds present, p , as a function of Φ/Φ_0 , we are able to obtain bounds for the S-N phase boundary. A very interesting mobility edge trajectory is found for the metal-to-insulator transition, which may be observable experimentally.

To examine the problem of the superconducting networks theoretically, we study the linearized Ginzburg-Landau (GL) equations appropriate near the phase boundary. For a network with current conservation at the nodes or lattice points,^{1-3,10}

$$-\Delta_i \sum_j \cot(\Theta_{ij}) + \sum_j \Delta_j e^{i\gamma_{ij}} / \sin(\Theta_{ij}) = 0 \quad (1)$$

where Δ_i is the order parameter at node or site i , $\Theta_{ij} = L_{ij}/\xi$ is the distance between nodes divided by the coherence length ξ , and $\gamma_{ij} = (2\pi/\Phi_0) \int_{ij} \mathbf{A} \cdot d\mathbf{l}$ is the circulation of the vector potential \mathbf{A} along the link ij . Equation (1) is, in general, difficult to solve but becomes more tractable for simple geometries. For regular networks which have links of equal length, i.e., $L_{ij} = L$, the $\sin(\Theta_{ij})$ term can be removed from the sum in Eq. (1), and the problem reduces to that of an electron on a similar lattice in a magnetic field.^{1-3,12}

For simple lattices, Eq. (1) can be written as

$$-\Delta_i z_i \cos\left(\frac{L}{\xi}\right) + \sum_{j=1}^{z_i} \Delta_j e^{i\gamma_{ij}} = \lambda \Delta_i \quad (2)$$

where the sum j is over the z_i nearest-neighbors of node site i and λ is the eigenvalue, which for the superconducting networks is equal to zero. Notice that Eq. (2) is very similar to the tight binding Hamiltonian of an electronic problem. However, here we are most interested in the zero eigenvalue case and the diagonal term depends on z_i and $\cos(L/\xi)$, which is taken to be equal to E . One way in which disorder can be introduced into Eq. (2) is by randomly removing $(1-p)$ of the sites, i.e., a fraction p of the sites or nodes are present. A link ij is present if only both nodes i and j are present. The system produced this way is called the site percolating system. Another way is by randomly removing $(1-p)$ of the bonds, so only a fraction of p bonds are present. This system is called the bond percolating system. To have a clear picture of the system we are dealing with, it helps to think that Eq. (2) is the eigen-equation with the eigenvalue $\lambda=0$ for a tight binding system with a diagonal energy $\epsilon_i = -E \cdot z_i$ and an off-diagonal hopping term $V_{ij} = t_{ij} \exp(i\gamma_{ij})$, where $t_{ij}=1$ if a link (or bond) between nodes i and j exists, and $t_{ij}=0$ otherwise. In this model the off-diagonal disorder is correlated with the diagonal one since the value of ϵ_i depends on z_i which is the sum of $|t_{ij}|$. To make the connection⁸ with the superconducting $T_c(H)$, it is usually assumed that $\xi = \xi_0(1-t)^{1/2}$, where $t = T/T_c(0)$ and, therefore $L/\xi = L(1-t)^{1/2}/\xi_0$. $T_c(H)$ can then be determined from the largest value of E for which Eq. (2) has a solution for $\lambda = 0$. In order to find the eigenvalues and eigenvectors, Δ_i , for Eq. (2), one can either diagonalize the Hamiltonian for a given H and p , or use the transfer matrix method and

finite-size scaling.^{13,14} This latter method is useful, since it can be used to study the nature of the different eigenstates, Δ_i , in particular, whether they are localized or extended. Direct diagonalization or a tridiagonalization procedure could be also used to study the nature of eigenstates, but is known not to give very accurate results.

In the transfer-matrix method,^{13,14} one considers coupled one-dimensional (1D) systems. Each 1D system is described by a tight binding Hamiltonian of the same form as Eq. (2). The corresponding sites of the nearest neighbor 1D system are coupled together by an interchain matrix element, $t_{ij}\exp(i\gamma_{ij})$, that depends on the strength of the magnetic field H and concentration p . In particular, we choose a gauge such that A is parallel to the 1D chains. For the site percolating system, we choose $t_{ij} = 1$ if both sites are present, δ if one site is missing, and δ^2 if both sites are missing. δ is very small compared with 1. For the bond percolating system, we choose $t_{ij}=1$ if a bond is present from i to j and $t=\delta$ otherwise. In Fig. 1, a random site percolating superconducting network is shown with the identifications of the different parameters. In the present work, M chains are coupled together into a 2D array with interchain coupling t_{ij} and $z_i = \sum_j t_{ij}$. The additional term t_{ij} is necessary for the transfer matrix method to insure that the lattice is connected. For the M connected chains of length N , one determines the largest localization length λ_M as $N \rightarrow \infty$. From a plot of λ_M versus M , one can obtain the localization properties of the system.^{13,14} In particular,

by studying the scaling plots λ_M/M versus M , one obtains a reasonable estimate of the mobility edge trajectory. Exactly at the mobility edge, we also find $\lambda_M/M = 0.6$ in agreement with previous work,^{13,14} while for extended and localized states we have that λ_M/M versus M increases or decreases, respectively. For our studies here, we used M equal to 2 through 64 with N up to 10,000, and $\delta = 10^{-4}$. We found that our results were independent of ϵ provided that $\delta \leq 10^{-3}$.

In addition for a given H and p , we numerically¹⁵ calculated the density of states (DOS) to obtain the positions and widths of bands and gaps. With the DOS known, the finite-size scaling analysis was used to determine the nature of the eigenstates in the bands.

At $p = 1$, we have $z_1 = 4$ and Eq. (2) with $l=0$ can be transformed to the "incommensurate" 1D tight binding model. Its energy spectrum has been studied in great detail by Hofstadter.¹² The phase boundary of the perfect square lattice can be easily obtained.¹² In order to check our numerical methods, we have also calculated for $p = 1$ the phase boundary $T_c(H)$. As can be seen from Fig. 2, the largest value of E which satisfies Eq. (2) for $\lambda = 0$ and is assumed to be proportional to the critical temperature $T_c(H)$ is plotted versus Φ/Φ_0 . Excellent agreement is found with previous works on the site percolating network.^{10,12} Along the y-axis, we plot $E = \cos(L/\xi)$, which is usually related to $T_c(H)$ through the relation $\xi = \xi_0(1-T/T_c(0))^{1/2}$, and, therefore, $L^2\{1-[T_c(H)/T_c(0)]\}/\xi_0^2 = (\arccos(E))^2$. The $T_c(H)$ shows all the interesting oscillations expected at rational values of Φ/Φ_0 . As we can see, the results for site percolation networks (Fig. 2a) and for

bond percolation networks (Fig. 2b) are quantitatively similar. The phase boundary $T_c(H)$ is numerically obtained with three independent methods which quantitatively agree with each other: (1) by a partial diagonalization of $10,000 \times 10,000$ matrix for a given H , and p to find the largest value of E for which $\lambda = 0$, (2) by the numerical calculation of DOS¹⁵ from which we can follow the behavior of the band edge of the highest band, and (3) by calculating the localization length with the finite-size scaling transfer matrix techniques.

For both site and bond diluted square lattice networks (i.e., $p_c < p < 1$, where $p_c = 0.59$ and $p_c = 0.5$ are the site and bond percolation threshold for the square lattice, respectively), we find the structure seen in E for $p = 1$ washed out even when $p = 0.90$ as seen in Fig. 2(a) and Fig. 2(b). Notice, when $p = 0.80$, all structure in E has disappeared.¹⁶ Below we will show, after examining the nature of the eigenstates D_1 which correspond to this particular value of E , that this simple mapping from E to $T_c(H)$, which was discussed above for $p = 1$ is not correct for $p < 1$ and determination of the phase boundary is actually more complex.

We have undertaken a systematic study of the extended or localized nature for all the eigenstates as a function of E . We found that the eigenstate corresponding to the largest value of E is not always extended, as has been implicitly assumed, in determining the phase boundary $T_c(H)$ in Fig. 2. Obviously if the Δ_1 are not extended, the solution with the largest eigenvalue cannot correspond to a superconducting state as occurs for $p = 1$. For $1 > p > p_c$ there exists

a mobility edge between localized and extended states. The actual value of $T_c(H)$ must then depend on the solution of the nonlinear Landau-Ginzburg equations and cannot be determined from the linearized equations. Because the nonlinear term can couple different localized eigenstates, the mobility edge trajectory found here can only be a lower bound of $T_c(H)$.¹⁷ In Fig. 3, we show for the site percolating networks whether the eigenfunctions are either localized or extended for several values of p and ϕ/ϕ_0 from which one can easily determine the upper and lower limits of $T_c(H)$. The energy at which the first solution appears gives the upper bound, while the energy for the first extended solution gives the lower bound. The $p = 1$ results agree very well with those of Ref. 12. For example, for $\phi/\phi_0 = 1/3$ and $p = 1.0$, we have three bands. However, since we only show $E > 0$, only the one band around $E = 0.8$ and half of the band around $E = 0$ are shown. The eigenstates for $p = 1$ are all extended. Notice that as p decreases for a given ϕ/ϕ_0 , we first lose some of the gaps that were present at $p = 1$ and then localized states begin to appear due to the site dilution. As the disorder increases, we find that all the states become localized. This is the case for $p = 0.60$, where, for all the magnetic field strengths studied, the eigenstates for all E are localized. However, for intermediate concentrations p , a rich and interesting behavior is obtained. Notice that for $\phi/\phi_0 = 1/3$ and $E = 0.3$, there is no eigenstate at this energy, for $p = 1$ case, the state is in a gap, while for $p = 0.90$ a localized state exists. It is very interesting that as disorder increases, we recover extended states at $E = 0.30$ for $p = 0.80$

and $p = 0.70$. This is contrary to one's usual intuition from which one expects localized states to appear as disorder increases. This unusual behavior occurs for the disordered superconducting network, because there is a competition between the disorder and the strength of magnetic field in determining the nature of the eigenstates. By diluting the system, we of course introduce more disorder, but the magnetic flux plaquettes rearrange themselves in such a way that an extended eigenstate remains. It would be very interesting to check this rich structure of mobility edge trajectories experimentally. For a given value of Φ/Φ_0 and given p , it might be possible to observe a metal-to-insulator type transition by changing E which effectively means changing temperature. For our particular superconductivity model, given by Eq. (2), the classical and the quantum percolation thresholds are exactly the same p for $H = 0$. This is due to the fact that the site energy, $z_1 \cos(L/\xi)$, is proportional to the number of nearest neighbors. Therefore, for $H = 0$, the $E = \cos(L/\xi) = 1$ eigenstate is always extended provided that $p \geq p_c = 0.59$.

Another interesting consequence of our results is that we can determine how the slope of the critical field depends on $p - p_c$, $(dH_{c2}/dT)_{T_c} \sim (p - p_c)^{-k}$ for $p > p_c$. For percolation, the linearized GL theory predicts that the critical exponent $k = \nu\theta$, where ν is the correlation length $\xi \sim (p - p_c)^{-\nu}$ exponent and θ is the anomalous diffusion exponent.⁸ This k value is expected not to depend on whether the system is site diluting or bond diluting. Taking $\nu = 4/3$ and $\theta = 0.8$ gives $k = 1.06$ in reasonable agreement with the numerical work on

linearized GL theory of Ref. 10 who found $k = 0.93$. Experimental values of $k = 0.57$ and $k = 1.06$ are given in Refs. 18 and 8, respectively, while Ref. 3 gives $k = 0.87$. To compare our results with previous work on random percolating networks, we have analyzed the initial part of $\Phi/\Phi_0 \leq 0.1$ of the phase boundary with the formula $H_{c2}(T) = A(1-t)\Phi_0/\xi_0^2$, where $t = T/T_c$. There $A = (\xi_0^2 T_c / \Phi_0) (dH_{c2}/dT)_{T_c}$. In Fig. 4, we plot A as a function of $p - p_c$ on logarithmic axis, for both the site and the bond diluting systems. Notice that A appears to vary with p for wide ranges of $p - p_c$. In Fig. 3, the triangles represent the largest value of E for which Eq. (2) has a solution for $\lambda = 0$, while the solid circles represent the eigenstate E (or temperature T_c) at which the first extended state appears as we reduce E . The extended curve is closer to the experiments,⁸ which is done for a bond diluting network. Notice that the exponent k for the extended curve is equal to 0.84 while for the band edge curve, $k = 1.70$ for both site and bond percolation networks which is much higher than the numerical estimations of Ref. 10 which give a value of $k = 0.93$. The open circles are the experimental data for A versus $p - p_c$ obtained by Ref. 8. Notice that the experimental data lie in between the two numerical predictions, which only give bounds to the real $T_c(H)$ suggesting that the agreement for the value of k given in Ref. 8 with the earlier prediction¹⁰ of the linearized GL theory is fortuitous. To determine the actual $T_c(H)$, the nonlinear terms which have been neglected in the present mean field treatment have to be taken into account.¹⁷ This breakdown of mean-field theory and the importance of nonlinear terms in

determining $T_c(H)$ probably explains the lack of dimensional crossover which was theoretically expected but not observed⁸ in percolating superconducting networks.

Conclusions

In conclusion, we showed that the linearized GL theory can not be used to determine the S-N phase boundary for disordered systems. It can only be used to bound the phase boundary. In cases of weak disorder, it probably gives a very good estimate of $T_c(H)$, but cannot be trusted for strong disorder. Instead, it is necessary to take account of the nonlinear terms which have been neglected in the linearized theory. We found that the cusplike structures present at $p = 1$ for $T_c(H)$ versus H are washed out for $p \leq 0.90$. The extended or localized nature of the eigenstates was also examined. A rich and interesting structure of mobility edge trajectories was obtained. Finally, the critical exponent of the upper critical field was calculated and found to be $1.7 > k > 0.84$, consistent with the experimental measurements.⁸

Acknowledgments

We acknowledge useful discussions with P. M. Chaikin, A. M. Goldman, J. M. Gordon and D. Levine. We also thank J. M. Gordon for sending us unpublished data that were used in Fig. 4. Ames Laboratory

is operated for the U.S. Department of Energy by Iowa State University under Contract No. W-7405-Eng-82. This investigation was supported by the Director for Energy Research, Office of Basic Energy Sciences. This work was partially supported by a Northwest Area Foundation Grant of Research Corporation.

References

1. P. G. de Gennes, C. R. Acad. Sci. B 292, 9, 279 (1981).
2. S. Alexander, Phys. Rev. B 27, 1541 (1983); S. Alexander and E. Haleri, J. Phys. (Paris) 44, 805 (1983).
3. R. Rammal, T. C. Lubensky, and G. Toulouse, Phys. Rev. B 27, 2820 (1983); J. Phys. Lett. 44, 65 (1983).
4. B. Pannetier, J. Chaussy, and R. Rammal, J. Phys. Lett. (Paris) 44, L853 (1983).
5. B. Pannetier, J. Chaussy, R. Rammal, and J. C. Villegier, Phys. Rev. Lett. 53, 1845 (1984).
6. J. M. Gordon et al., Phys. Rev. Lett. 56, 2280 (1986).
7. A. Behrooz et al., Phys. Rev. Lett. 57, 368 (1986); Phys. Rev. B 35, 8396 (1987).
8. J. M. Gordon, A. M. Goldman, and B. Whitehead, Phys. Rev. Lett. 59, 2311 (1987).
9. S. P. Benz, M. G. Forrester, M. Tinkham, and C. J. Lobb, Phys. Rev. B 38, 2869 (1988).
10. J. Simonin and A. Lopez, Phys. Rev. Lett. 56, 2644 (1986).

11. Y. Y. Wang, R. Rammal, and B. Pannetier, J. Low Temp. Phys. 68, 301 (1987).
12. D. R. Hofstadter, Phys. Rev. B 14, 2239 (1976).
13. C. M. Soukoulis, E. N. Economou, and G. S. Grest, Phys. Rev. B 36, 8649 (1987); A. D. Zdetsis et al., Phys. Rev. B 32, 7811 (1985), and references therein.
14. J. L. Pichard and G. Sarma, J. Phys. C 14, L127 (1981); A. Mackinnon and B. Kramer, Phys. Rev. Lett. 47, 1546 (1981); Z. Phys. B 53, 1 (1983).
15. Qiming Li, C. M. Soukoulis, and E. N. Economou, Phys. Rev. B 37, (1988).
16. This is in disagreement with Ref. 9 where some structure is still seen even at $p = 0.70$. We believe that the three independent numerical methods used in our study to find the largest eigenvalue is superior to the tridiagonalization technique used in Ref. 9. Most probably the continued fractions used in 512 iterations⁹ did not give the correct E . It appears that for $p < 1$, Ref. 9 always overestimates E and that is why some structure of E remains even at $p = 0.70$.
17. J. A. Hertz, Phys. Rev. Lett. 51, 1880 (1983); A. J. Bray and M. A. Moore, J. Phys. C 15, L765 (1982) have observed similar behavior in spin glasses.
18. G. Deutscher, I. Grave, and S. Alexander, Phys. Rev. Lett. 48, 1497 (1982).

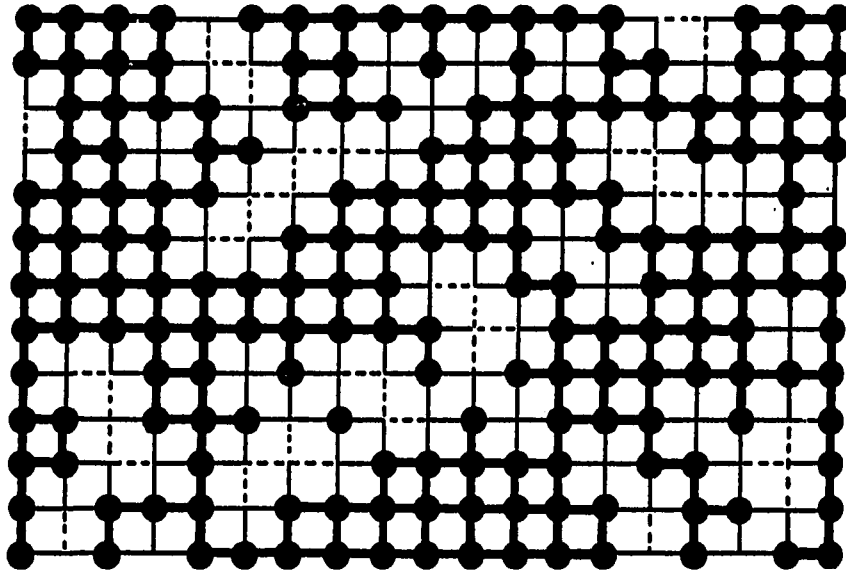


Fig. 1. Random percolating superconducting network with the fraction p of the sites present equal to 75%. The nearest neighbor matrix element $t_{ij} = 1$ (*—*), δ (*—) or δ^2 (---) if both, one or zero sites are present, respectively.

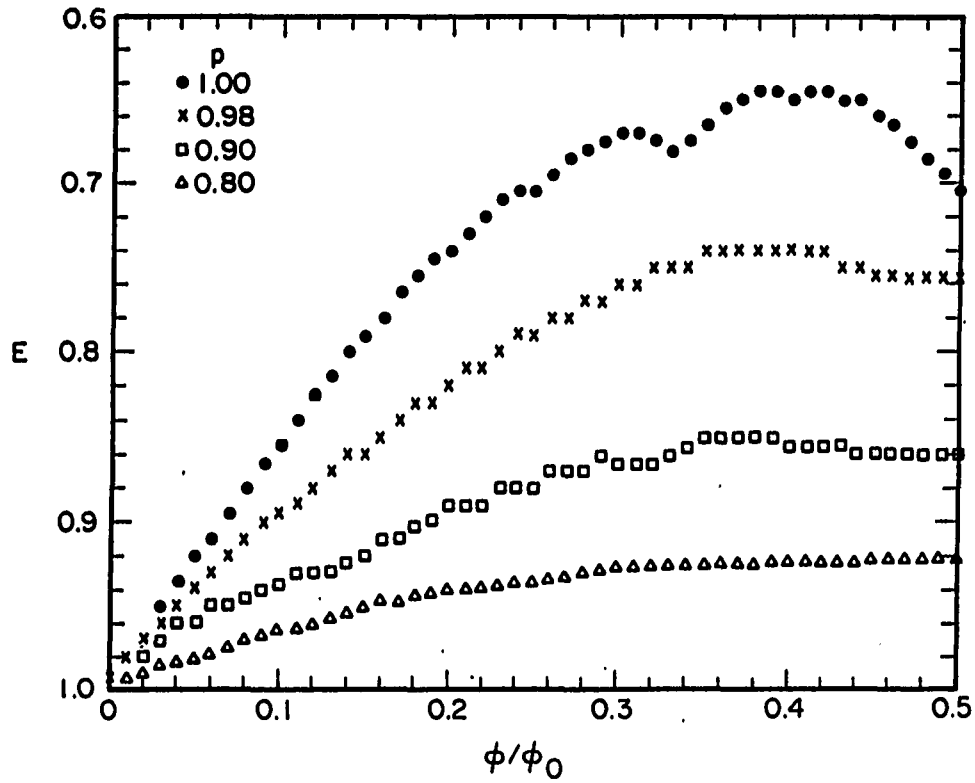


Fig. 2a. Phase boundary of the percolating superconducting square network for site concentrations $p = 1, 0.98, 0.90$, and 0.80 . The y-axis represents the largest eigenstate E , while the x-axis represents ϕ/ϕ_0 , where $\phi = L^2 H$ is the magnetic flux through the unit cell and ϕ_0 is the superconducting flux quantum

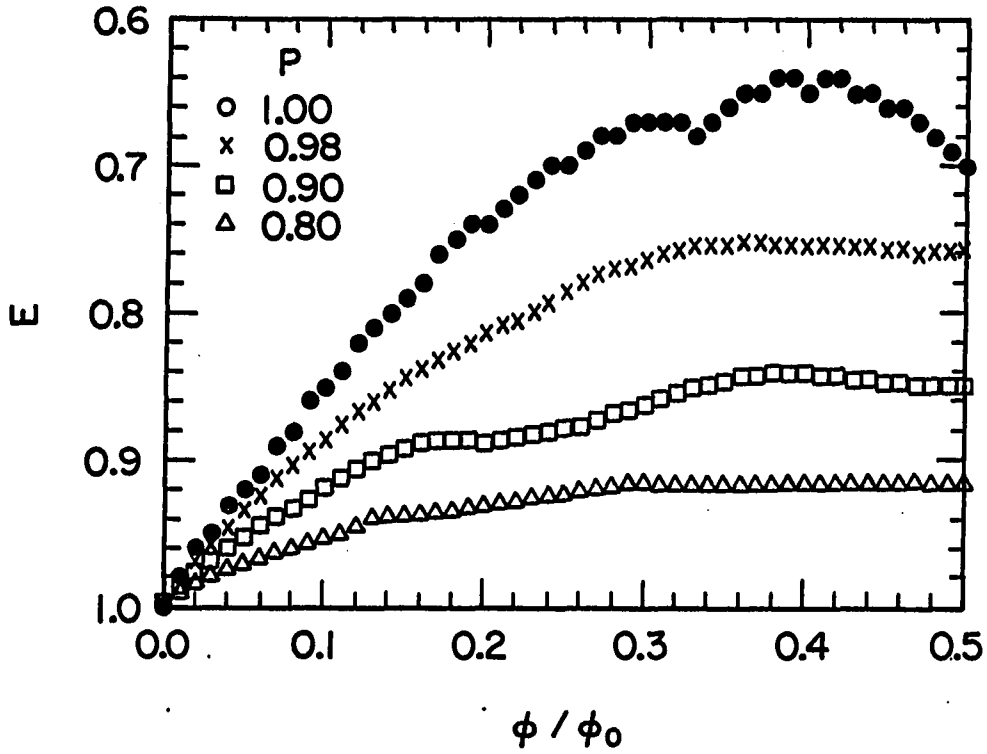


Fig. 2b. Phase boundary of the percolating superconducting square network for bond concentrations $p = 1, 0.98, 0.90$, and 0.80 . The y-axis represents the largest eigenstate E , while the x-axis represents ϕ / ϕ_0 , where $\phi = L^2 H$ is the magnetic flux through the unit cell and ϕ_0 is the superconducting flux quantum

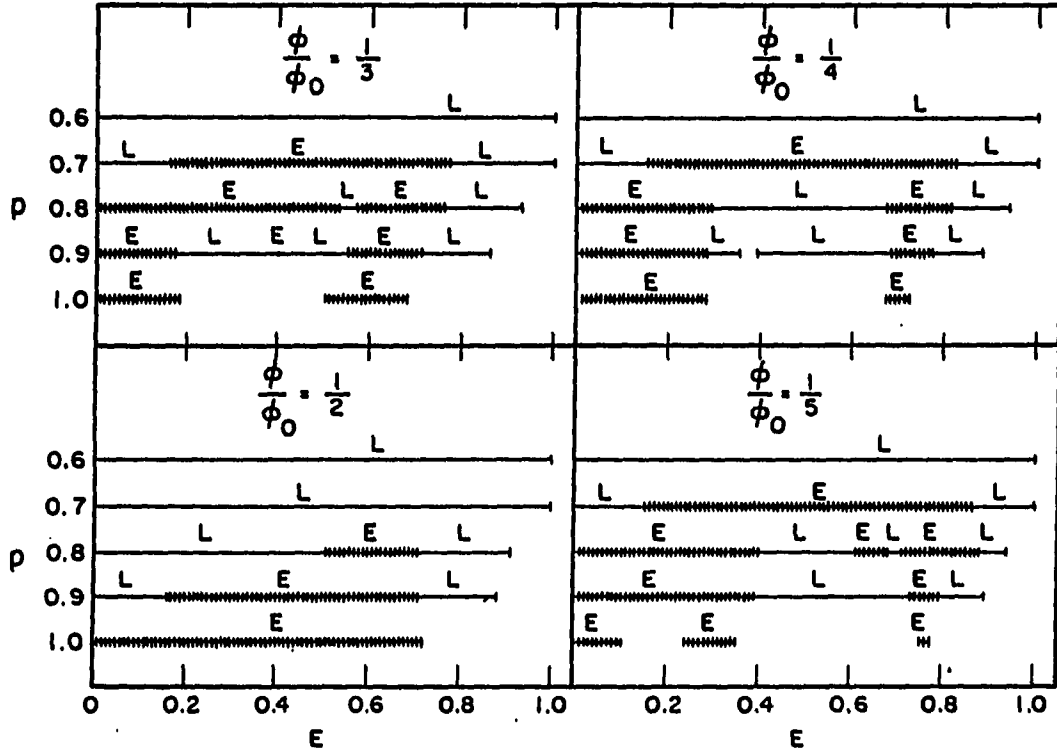


Fig. 3. The concentration dependence of the eigenstates E for different magnetic fields $\phi/\phi_0 = 1/2, 1/3, 1/4$, and $1/5$. The symbols E and L represent extended and localized states, respectively. For a given p , (—), (+++), and (blank space) represent localized, extended, and no states, respectively.

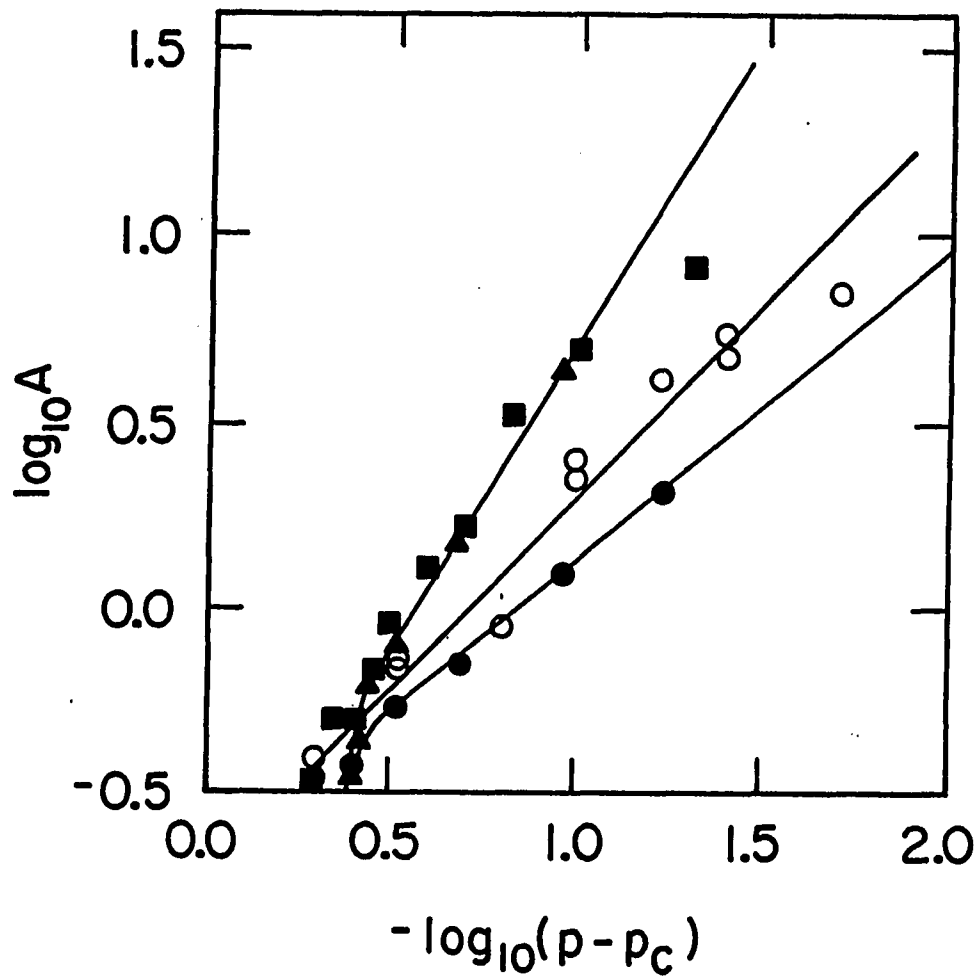


Fig. 4. Log-log plot of parameter $A \sim dH_{c2}/dT$ versus $p - p_c$ for the site percolation band edge (\blacktriangle), bond percolation band edge (\blacksquare), and first extended states (\bullet) for site percolation from our numerical calculations. The experimental results (\circ) of Ref. 8 for bond percolation are also presented.

SUMMARY

Magnetic flux effects provide an ideal tool to study the quantum conductance of disordered materials. In this dissertation we presented the theoretical studies of the magnetic flux effects on disordered small normal metal rings and on random superconducting networks. Parts I and II are aimed at the understanding of the quantum conductance oscillations in mesoscopic systems, such as normal metal rings. In Part I, we studied analytically the transmission coefficient of a one-dimensional ring under magnetic field by using the scattering matrix method. The conductance was then related to the transmission coefficient using the Landauer's formula. We found that an ensemble average over the phase of the scattering centers changes the period of the conductance oscillation from h/e to $h/2e$. This important finding shined some light on the origin of the AAS effect. This result is obtained for a strictly one-dimensional rings. In Part II, through the calculation of the localization length for small rings with a finite width and a series of rings, we showed that the dominant oscillations of the conductance in a single configuration is of the h/e period, but either the ensemble average or the self-average due to the large number of rings, will make the h/e component disappear and change the period of the conductance oscillation to $h/2e$ (AAS type), in agreement with the results obtained in Part I. We also found an unexpected universal law for the oscillation of localization length. The expected universal fluctuation amplitude at weak disorder was observed. The much larger

amplitude of the fluctuations of the conductance in extremely weak disorder case shows possibilities of novel effects, possibly connected to the nonlocal effects observed in the experiments when phase coherence length is larger than the distance between the probes.

In Part III, the nature of the states on normal-to-superconducting phase boundary for two-dimensional random superconducting networks are studied through the finite-size scaling transfer matrix calculation within the mean-field Ginzburg-Landau theory of second-order phase transition. A rich structure for the mobility edge was obtained. The existence of two different phase boundaries, one for the band edge and the other for the first mobility edge, may have important experimental consequences. If the true transition boundary is indeed not the band edge state but within the band, then nonlinear Ginzburg-Landau has to be studied.

In conclusion, we have studied the magnetic flux effect on both disordered normal metal rings and random superconducting networks, with an emphasis on the quantum coherence of electrons and the localization nature in the disordered systems.

LITERATURE CITED

1. For a review, see P. A. Lee and T. B. Ramakrishnan, Rev. Mod. Phys. 57, 287(1985); B. L. Al'tshuler and P. A. Lee, Physics Today, 41, 36 (1988)
2. P. W. Anderson, Phys. Rev. 109, 1492 (1958).
3. N. F. Mott, Adv. Phys. 16, 49 (1967) and N. F. Mott, Phil. Mag, 17, 1259 (1968).
4. D. J. Thouless, Phys. Rep. 12, 93 (1974); Phys. Rev. Lett. 39, 1167 (1977); J. T. Edwards and D. J. Thouless, J. Phys. C. 5, 807 (1972); D. C. Licciardello and D. J. Thouless, Phys. Rev. Lett. 35, 1475 (1975).
5. E. Abrahams, P. W. Anderson, E. C. Licciardello, and T. V. Ramakrishnan, Phys. Rev. Lett. 42, 673 (1979).
6. A. Mackinnon and B. Kramer, Phys. Rev. Lett. 47, 1546 (1981)
7. G. Bergmann, Phys. Rep. 107, 1 (1984).
8. R. Landauer, IBM J. Res. Dev. 1, 223 (1957).
9. P. W. Anderson, D. J. Thouless, E. Abrahams, and D. S. Fisher, Phys. Rev. B 22, 3519 (1980).
10. E. N. Economou and C. M. Soukoulis, Phys. Rev. Lett. 46, 618 (1981); D. S. Fisher and Patrick A. Lee, Phys. Rev. B 23, 6851 (1981); also see I. M. Lifshits et al., Introduction to the Theory of Disordered Systems (John Wiley & Sons, Inc., New York, 1988).

11. M. Buttiker, Phys. Rev. Lett. 57, 1761 (1986).
12. A. D. Stone, Phys. Rev. Lett. 54, 2692 (1985).
13. J. C. Licini, D. J. Bishop, M. A. Kastner, and J. Melngailis, Phys. Rev. Lett. 55, 2987 (1985).
14. R. A. Webb, S. Washburn, C. P. Umbach, and R. B. Laibowith, Phys. Rev. Lett. 54, 2696 (1985).
15. S. Datta, M. Rmelloch, S. Bandyopadhyay, R. Noren, M. Varizi, M. Miller, and R. Reifenberg, Phys. Rev. Lett. 55, 2344 (1985).
16. P. A. Lee and A. D. Stone, Phys. Rev. Lett. 55, 1622 (1985); P. A. Lee, A. D. Stone, and B. L. Al'tshuler, JETP Lett. 41, 648 (1985); B. L. Altshuler and B. I. Shklovskii, Sov. Phys. JETP 6, 127 (1986); P. A. Lee, A. Stone, and H. Fukuyama, Phys. Rev. B 35, 1039 (1987).
17. Y. Imry in Direction in Condensed Matter Physics G. Greistein and E. Mazenko, eds. (World Scientific, Singapore, 1986); A. D. Stone and Y. Imry, Phys. Rev. Lett. 56, 189 (1986).
18. See reviews, C. V. Haesendonck et al., Physica Scripta, T19, 87 (1987); W. J. Skocpol, Physica Scripta T19, 95 (1987).
19. W. J. Skocpol et al., Phys. Rev. Lett. 58, 2343 (1987); A. Beroit et al., Phys. Rev. Lett. 58, 2347 (1987).
20. A.D. Benoit, S. Washburn, C. P. Umbach, R. B. Laibowitz, and R. A. Webb, Phys. Rev. Lett. 57, 1765 (1986).
21. Y. Aharonov and D. Bohm, Phys. Rev. 115, 485 (1959).
22. B. L. Al'tshuler, A. G. Aronov, and B. E. Spivak, JETP Lett. 33, 94 (1981).

23. D. Y. Sharvin and Y. V. Sharvin, JETP Lett. 34, 272 (1981).
24. V. Chandrasekhar, M. Rooks, S. Wind, and D. Prober, Phys. Rev. Lett. 55, 1610 (1985).
25. M. Buttiker, Y. Imry, and R. Landauer, Phys. Lett. 96A, 365 (1983); M. Buttiker, Y. Imry, and M. Azbel, Phys. Rev. A 30, 1982 (1984); M. Buttiker, Y. Imry, R. Landauer, and S. Pinhas, Phys. Rev. B 31, 6207 (1985); Y. Gefen, Y. Imry, and M. Azbel, Phys. Rev. Lett. 52, 129 (1984).
26. Qiming Li and C. M. Soukoulis, Phys. Rev. B 33, 7318 (1986).
27. C. P. Umbach, C. Van Haesendonck, R. B. Laibowitz, S. Washburn, and R. A. Webb, Phys. Rev. Lett. 56, 386 (1986).
28. Qiming Li and C. M. Soukoulis, Phys. Rev. Lett. 57, 3105 (1986).
29. F. London, Phys. Rev. 74, 562 (1948).
30. N. Byers and C. N. Yang, Phys. Rev. Lett. 7, 46 (1961); L. Onsager, Phys. Rev. Lett. 7, 50 (1961).
31. B. S. Deaver and W. M. Fairbank, Phys. Rev. Lett. 7, 43 (1961).
32. W. A. Little and R. D. Parks, Phys. Rev. Lett. 9, 9 (1962).
R. D. Parks and W. A. Little, Phys. Rev. 97A, 133 (1964).
33. See for example, Allen M. Goldman and S. A. Wolf, eds., Percolation, Localization, and Superconductivity (Plenum Press, New York, 1984).
34. D. Stroud and W. Y. Shih, Mater. Sci. Forum 4, 177 (1985).
35. P. G. de Gennes, C. R. Acad. Sci. B 292, 9 (1981); P. G. de Gennes, C. R. Acad. Sci. B 292, 279 (1981); S. Alexander, Phys. Rev. B 27, 1541 (1983).

36. J. M. Gordon et al., Phys. Rev. Lett. 56, 2280 (1986).
37. J. M. Gordon, A. M. Goldman, and B. Whitehead, Phys. Rev. Lett. 59, 2311 (1987).
38. D. R. Hofstadter, Phys. Rev. B 14, 2239 (1986).
39. Qiming Li, C. M. Soukoulis, and E. N. Economou, Phys. Rev. B 37, 8289 (1987) and references therein.
40. J. M. Gordon, A. M. Goldman, and B. Whitehead, Phys. Rev. B 38, 12019 (1988).
41. C. M. Soukoulis, G. Grest, and Qiming Li, Phys. Rev. B 38, 12000 (1988)

ACKNOWLEDGMENTS

I would like to express my deepest gratitude to my dissertation advisor, Dr. Costas M. Soukoulis, for his constant help, guidance, and encouragement. It has been my great pleasure during the course of the past years to work closely with him on several interesting topics. I have benefited from him both as a supervisor and as a friend.

I sincerely thank the members of my committee: Drs. M. Luban, B. L. Young, Ed Wolf, R. Trivedi and M. Tringides for their encouragement and support. I am especially grateful to Dr. Ed Wolf for initially suggesting for me to study the Aharonov-Bohm effect in metal rings. Collaborations with Dr. G. S. Grest on Metal-Insulator transitions in random superconducting networks are gratefully acknowledged.

Last, but not least, I would like to thank my parents and my wife for their unfailing support and encouragement throughout my years at Iowa State University.

This work was performed at Ames Laboratory under contract No. W-7405-eng-82 with the U. S. Department of Energy. The United States government has assigned the DOE Report number IS-T-1388 to this dissertation.

APPENDIX. NUMERICAL METHOD OF FINITE SIZE SCALING

Due to the difficulty of dealing with large systems numerically, Mackinnon and Kramer¹⁶ introduced a new technique to study the disordered system based on renormalization ideas. In this technique, we obtain first the localization length λ_M for a quasi-one-dimensional strip or bar with finite width M through a recursion relation of Green's function. A finite λ_M is always obtained this way because the system is one-dimensional and all states are localized. We calculate λ_M for many M up to the maximum M the computer time is allowed. The nature of the eigenstates can be determined by the behavior of λ_M : if λ_M increases faster than M , then the state is extended; if λ_M increases slowly with M and then saturates for large M , the state is localized. To get the localization length for the infinite system, we simply force all the numerical data into a universal curve by choosing a characteristic length ξ for all M and for that particular energy and disordered strength, i.e.,

$$\Lambda(M, E, W) = f_d\left(\frac{\xi(E, W)}{M}\right), \quad (A.1)$$

where $\Lambda = \lambda_M/M$ and W represents the strength of disorder. ξ has the meaning of localization length in the localized region and coherent length in the extended region.

The scaling function can be defined as

$$\chi(\ln \Lambda) = \frac{d \ln \Lambda}{d \ln M} \quad . \quad (A.2)$$

For small Λ , we expect $\xi \sim \lambda_M$. Hence,

$$\chi(\ln M) = -1 \quad (A.3a)$$

$$\Lambda(M, E, W) = \xi(E, W)/M \quad (A.3b)$$

$$f(x) = x \quad . \quad (A.3c)$$

For large Λ , identifying ξ as the inverse of the conductivity,⁶ we get

$$\lambda_M \sim W^{-2M^{d-1}} \quad (A.4a)$$

$$\chi(\ln \Lambda) = d-2 \quad (A.4b)$$

$$\Lambda(M, E, W) = (M/\xi(E, W))^{d-2} \quad (A.4c)$$

$$f(x) = x^{2-d} \quad . \quad (A.4d)$$

From these analyses, localization lengths and mobility trajectories can be accurately determined. This finite size scaling method is still the most reliable method up to now to numerically study the localization phenomena in disordered systems.